OPTIMISING THE PERFORMANCE OF DOMESTIC WALL MOUNTED SPACE COMFORT HEATER

by

Jerome Tangkeh Njofang

Dissertation submitted in partial fulfilment of the requirements for the degree

Master of Technology: Mechanical Engineering

in the Faculty of Engineering

at the Cape Peninsula University of Technology

Supervisor**: Prof Jasson Gryzagoridis**

Bellville Campus

Date submitted**: September 2016**

DECLARATION

I, **Jerome Tangkeh Njofang**, declare that the contents of this dissertation represent my own unaided work, and that this dissertation has not previously been submitted for academic examination towards any qualification. Furthermore, it represents my own opinions and not necessarily those of the Cape Peninsula University of Technology.

_____   _____

                Signature   Date

ABSTRACT

The performance of a wall Mounted space comfort heater has been studied with respect to the geometry of its mounting condition. Tests were conducted in a laboratory with the heater positioned at various heights from the floor and the channel that is created by the various gaps with the wall on which the heater was mounted. Tests were also performed with the heater mounted on the wall whose emissivity was adjusted to low, medium and high values as well as placing insulation material on the wall directly behind the heater. The outcome of the experiments revealed an acceptable geometry of the heater's mounting at least 200 mm above the floor, and 50 mm off-set from the wall. The results of the heater mounted against the wall revealed a drop in performance as compared to the heater's "benchmark" performance when it was freely standing on the floor of the laboratory; with an efficiency of about 41% (almost evenly shared by each face). This efficiency, which is based on the convective heat transfer generated by the heater's warm/hot surfaces, is relative to the electrical energy input and it dropped when the heater was mounted against a grey wall to around 35%, of which only 26% was produced inside the channel. The heat transfer by radiation from the heater's surface is treated as net loss to the walls of the room/enclosure.The performance of the heater when mounted against the wall improved almost to the benchmark value when the wall behind the heater was made refelective (low emissivity). It is recommended that further research should be undertaken to thoroughly investigate the "mode" of heat transfer, by the induced flow through the channel, in a more formal or scientific modelling approach.

ACKNOWLEDGEMENTS

I wish to thank:

DEDICATION

This humble work is dedicated to my Grand-Mother, the Late Tankeu Anne (1918-1998) of Bangangte in Cameroon, who early instilled in me the principle that: the future value of a man is rooted in his perpetually growing intellectual capabilities and these capabilities were to confidently serve as his own solid brick laid in the edification of a responsible living society and a reassuring anchor for a strong and sustainable family life.

GLOSSARY

ABBREVIATIONS

Av	Average
Chan	Channel between heater and wall
Channel	Gap left between the heater and the wall
Cond	Conduction (heat transfer)
Conv	Convection (heat transfer)
HT	Heat Transfer
Inlet	At the entry of the channel
Inner	Surface of the heater facing the wall
Outer	Surface of the heater facing the rest of the enclosure
Outlet	At the exit of the channel
Q_{out}	Rate of heat transfer from the surface of the heater facing the rest of the enclosure
Rad	Radiation (heat transfer)
Temp	Temperature
T_{Film}	Average temperature between the heat source and the ambient
T_{inner}	Temperature at the surface of the heater facing the wall
T_{outer}	Temperature at the surface of the heater facing the rest of the enclosure
Tot	Total
v	Velocity
Wall	Wall against which the heater is mounted

NOMENCLATURE

A	Surface area of the heater (m^2)
A_1 and A_2	Surface areas 1 and 2 respectively (m^2)
A_c	Cross sectional area of the channel (m^2)
α	Coefficient of thermal diffusivity of air (Conductivity/(density x specific heat) in (m^2/s)
β	Coefficient of thermal expansion of air (1/K)
C_p	Heat capacity of air at a constant pressure (J/kg/K)
$C_{p_{inlet}}$	Specific heat capacity of air (J/kg/K)
ε_1 and ε_2	Emissivity of surfaces 1 and 2 respectively (dimensionless)
F_{12}	Form or Radiation heat transfer view factor between surface 1 and surface 2
Gr_L	Grashof number based on the characteristic length of the heater (dimensionless)
g	Gravitational constant (m/s^2)
h	Coefficient of convective heat transfer W/(m^2.K)
k	Coefficient of thermal conductivity of the air W/(m.K)

L	Characteristic length (height) of the heater (m)
$\dot{m}$	Mass flow rate of air going through the channel (kg/s)
Nu_L	Nusselt number based on the characteristic length of the heater (dimensionless)
Pr	Prandtl number (dimensionless)
Q_{12}	Net radiation heat transfer between surface 1 and surface 2 (W)
$\dot{Q}_{Cal}$	Calorimetric HT through the channel (W)
$\dot{Q}_{Conv}$	Total convection heat transfer from the heater's surface (s) (W)
Ra_L	Rayleigh number based on the characteristic length of the heater (dimensionless)
ρ_{inlet}	Density of air at the inlet (bottom) of the channel (kg/m^3)
σ	Stefan-Boltzmann constant $\sigma = 5.67 \times 10^{-8}$ W m^{-2} K^{-4}
T_1 and T_2	Absolute temperatures of surfaces 1 and 2 (K)
T_∞	Enclosure's air temperature (K)
$T_{outlet} - T_{inlet}$	Temperature difference between the hot air exiting the channel and the fresh air entering it. (K)
T_s	Temperature of the heater's surface (K)
$(T_S - T_\infty)$	Temperature difference between the hot surface and the ambient (K)
μ	Absolute viscosity of air (kg/(m.s)) or (Pa/s)
ν	Kinematic viscosity of air (m^2/s)
ν_{inlet}	Velocity of air at the inlet (bottom) of the channel (m/s)

Table of Contents

List of Figures

List of Tables

CHAPTER 1

INTRODUCTION

1.1 Overview

This research was conducted on a wall mounted space comfort heater with a view to optimise its performance via the geometry of the heater's mounting as well as varying the surface conditions of the wall behind the heater. A space heater is a self-contained appliance for heating an enclosed space within a building. This means that the space heater mostly heats up first the air in the enclosure which in turn would provide comfort to users, rather than to deliver heat that is directly absorbed by clothing and skin. Wall mounted space heaters are normally mounted at a fixed position against the wall of the room's enclosure. They have been employed by many users because of their fixed position, as opposed to other heaters that need to be moved around to wherever the need for comfort arises. The mounting of a space heater against the wall is an attempt to make the heater useful and out of the way of the enclosure's occupants.

Early space heaters date back around the 14th century, like the Japanese Kotatsu [1] that was a heater built in the form of a table, which was improved around the 20th century as an electrically heating device. Space heaters underwent several improvements in their history; the first was invented around 1990 [2].

Figure 1-1:   Wall mounted space comfort heater

Wall mounted heaters like various other domestic appliances are used as partial but important solution to a household's need, their performance in heating up the environment air being a key factor in the satisfaction of the need.

The outcome of this research is viewed as a contribution towards improving the performance of a wall mounted heater which instinctively appears to be affected by the geometry of its mounting.

1.2   Problem statement

Some space heaters are equipped with fans that blow the air over the hot (in some instances glowing) surface of the heaters directly towards the surrounding air. This sometimes parallel radiant with forced convection heat transfer modes that such heaters offer, quickly satisfy the immediate needs of users. The high mobility of their positioning inside say the room of a house does signal the hazard of navigating around them or blocking humans' movements in confined spaces. Others like the one dealt with in this study, are located in an isolated position inside the room of a house, an office etc. and those are normally fixed against a wall. However, this mounting against the wall is likely to impact on the heater's performance and henceforth brings the need to research this arrangement.

1.3   Background of the problem

Wall mounted space heaters are mainly free convection heaters that use electrically heated ceramic covered elements for the warming of the room's air. They are usually designed for relatively small room areas (around $12m^2$) and may need some amount of time to reach the peak of their functionality, as they heat-up the air space of the enclosure to a suitable room temperature with low energy consumption (around 400W). They are also designed with a relatively flat (slim) rectangular shape that can easily be accommodated by the wall. With regards to other advantages, manufacturers point out that wall mounted space heaters' non-portability, combined with their slim shape and the fact that they are made of non-toxic materials and added to their silent mode of operation makes them sleep-friendly and hence perfect for hotels, homes and apartments, and also safer for children as well as elderly peoples' living facilities [3].

Wall mounted space heaters appear to experience some heat loss by conduction through the wall because the wall behind them gets considerably hotter than the rest of the enclosure. Their fixed position next to a wall creates a gap or channel, which is viewed as an interesting area for the overall heat transfer from the heater, as it includes 'convective' heat transfer to the enclosure's air and net radiation heat loss to the wall opposite the "inner" surface of the heater. The operational configuration of space heaters related to their mounting against the wall, comprises some geometric parameters likely to affect their performance, namely the

2

channel gap between the heater and the wall as well as the height of the heater above the floor.

1.3 Literature review

Analytical and experimental work regarding the phenomenon of heat transfer from a hot surface to a surrounding fluid, possibly in an enclosure where radiation heat transfer as well takes place, has been amply recorded in the relevant literature. More precisely, the heat transfer by natural convection from a heated vertical plate to the surrounding air has been studied in great detail.

The earlier work of heat transfer from vertical heated surfaces put into evidence the boundary layer theory [4]. A combined experimental and numerical approach applied to multi-mode heat transfer between vertical parallel plates has been performed with the aim to determine the significance of radiation's contribution to the total heat transfer rate on a steel plate in a relatively big channel gap and the validity of the isothermal surface assumption [5]. According to [6], an investigation of the natural convection heat transfer coupled with the effect of thermal conduction from a steel plate with discrete heat sources, was conducted, using the heat transfer and temperature distribution of the plate measured with different heating spaces. This led to two boundary conditions, with constant heating flux and temperature, determined by controlling the heat sources mounted on the back of the plate and correlating the heat transfer as a function of the relative heating space and the Rayleigh number. An experiment was conducted on the numerical analysis of the flow and heat transfer characteristics of buoyancy-driven air convection behind photovoltaic panels [7] to validate the effect of different input heat fluxes and emissivity of the bounding surfaces on the heat transfer across the air layer. Similarly in another experiment [8], validation of the predicted results for the mass flow rate, velocity, temperature rise and location of neutral height (location where the pressure in the air gap is equal to the ambient pressure) in air gaps behind solar cells located on vertical facades, was achieved by varying the geometry of the air gap and the location of the solar cell module.

1.4 Research objectives

The main objective of this research is to study aspects of this space heater's mounting conditions that may help improve its performance.
In order to achieve this objective, various tests for the evaluation of the overall heat transferred from the heater to the enclosure will be performed assuming isothermal heating of

the heater's surfaces and a power factor of unity for its electrical energy conversion. The total heat transferred from this heater will be compared to the total input electrical energy consumed. In addition to the above mentioned parameters, this research will also investigate the effects of surface properties of the wall behind the heater such as emissivity and insulation against conduction losses through the wall.

1.5   Research methodology

This section will consist of the followings:

- The design and manufacture of a mounting assembly or system that will handle the heater for various experiments to be performed at various geometries of this heater's mounting, as well as the design and manufacture of the insulation panel that will constitute the insulated wall behind the heater.
- The selection and description of various tools and devices that will constitute the instrumentation of the measuring system for data recording.
- The methodology for sequentially performing various tests as proposed below;

  - Conduct tests on the heater positioned vertically and freely inside the enclosure, for testing its performance that would serve as the bench mark for all the other tests.
  - Conduct tests on the heater which is mounted against the normal existing wall, under the geometric variation of the channel gap between the heater and the wall.
  - Perform tests on the heater mounted against the normal existing wall, under the geometric variation of the height between the heater and the floor of the room.
  - Study the effect of a low emissivity surface of the wall behind the heater.
  - Study the effect of high emissivity of the surface of the wall behind the heater.
  - Study the effect of insulation mounted on the wall behind the heater

Some of previous works found in the literature describe adequately the free convection heat transfer from a vertical plate, applicable in this study only to the heater's face exposed to the rest of the room. The other face, forming the channel with the wall, displays a configuration that does not appear to have been investigated previously. The flow of air is constrained in the channel and does not afford the opportunity for the interaction with fresh enclosure's air along the heater's characteristic length (height), only at the channel's entrance and exit at the bottom and the top of the heater respectively. In the absence of a classical solution to the heat transfer from this particular geometry, the author opted for the calorimetric approach which is

a practical approach to evaluate the heat transferred from the heater's surface forming the channel.

1.6 Research delineations

The specimen for the experiments will be made from two exactly the same well-known heaters (of model H400W Local Panel where one serves as a back-up to the other), which have been kindly provided by the manufacturer to be used for this study. No internal configuration of the heater will be explored in order to conform to the confidentiality and non-disclosure agreement that was signed between the manufacturer of the heaters and the Cape Peninsula University of Technology (CPUT).

This research is mainly conducted as mentioned initially, to check the effect of geometry as well as surface properties (emissivity and insulation) of the wall behind the heater, on the overall heat transferred from the heater's hot surfaces to the surrounding. For these reasons:

- Temperatures will be recorded from the hot surfaces of the heater and the wall behind it, and at their respective vicinities, as well as across the relatively narrow channel gap between the heater and the wall. The room temperature will be measured just for the sake of the determination of the film temperature, specifically for the heater's outer surface.

- The enclosure was assumed free from extraneous heat transfer but with relative air permeability through it. Consequently, there will be no significant variation of the room's temperature during the duration of experiments.

1.7 Expected outcomes

This research is projected to have the following possible outcomes:

1.7.1 Expected results

- Impact of the mounting of the heater against the wall on the overall heat transferred from the heater to the surroundings.
- Extent to which the gap variation of the heater from wall is likely to affect the overall heat transferred from the heater to the surroundings.
- Extent to which the height variation of the heater from floor is likely to affect the overall heat transferred from the heater to the surroundings.
- Extent to which the low emissivity (reflective) wall behind the heater is likely to affect the overall heat transferred from the heater to the surroundings.

5

- Extent to which the high emissivity (black) wall behind the heater is likely to affect the overall heat transferred from the heater to the surroundings.
- Extent to which the insulation on the wall behind the heater is likely to affect the overall heat transferred from the heater to the surroundings.

1.7.2   Expected significance of the research

The analysis and interpretations of results from 1.8.1 above should lead to the proposal of the eventual mounting conditions of the particular wall mounted heater that would perhaps optimise its performance.

1.7.3   Expected scientific contributions of the research

This research is envisaged to deduce the heat transfer process through a vertical channel with geometry and conditions that has not been previously investigated, thus promoting investigations towards an eventual formal scientific model solution.

1.8   Dissertation's outline

Chapter 1 comprised the proposal as well as the introduction to this research. In **Chapter 2** there is a detailed presentation of the theoretical background built-up from the relevant literature explored and applicable to the various conditions of the envisaged experimental work. The design and implementation methodology was postulated and executed in **Chapter 3**, with focus on the description of the materials gathered for the testing, design and manufacture of the testing equipment as well as the testing procedures. The analyses of the data as well as the results / interpretations are covered in **Chapter 4**. Concluding remarks and recommendations relevant to the topic are drawn in **Chapter 5**. References precede the tables of data, air properties of air, temperature conversion chart sample calculations etc., which are presented in the appendices.

1.9   Summary

A broad presentation of the research overview has been made in this introductory chapter, via the research problem statement, the background of the topic of investigation, a detailed literature explored, the methodology designed for the study as well as its expected outcomes. The dissertation outline has also been presented to conclude the chapter. The details of the outline will continue with Chapter 2 emphasising the theoretical background of the study.

CHAPTER 2

HEAT TRANSFER THEORY

2.1   Introduction

This chapter covers the theoretical background governing the process of heat transfer from the wall mounted space comfort heater, chosen for the purpose of this research. Two main areas of heat transfer considered are: i) the outer surface of the heater facing the rest of the room or enclosure and ii) the channel of heat flow created between the heater and the wall that it is mounted on.

As mentioned in the previous chapter, several modes of heat transfer are involved in the operation of the heater. The theoretical energy balance between the electrical energy input and the overall heat transfer resulting from the heater's operation incorporates the three components of heat transfer: conduction, convection and radiation. The theoretical energy balancing equation governed by the principle of energy conservation [9] could be written as:

$$Q_{Input} = Q_{Cond} + Q_{Conv} + Q_{Rad} .$$
(2-0)

Where,

Q_{Input} is the electrical power input to the heater (W)

Q_{Cond} is the total conduction heat transfer loss (W)

Q_{Conv} is the total convection heat transfer loss from the heater's surface (W)

Q_{Rad} is the total radiation heat transfer loss from the heater's surface (W)

The conduction heat transfer losses from the heater are negligible therefore the main focus will be on the convection and radiation modes of heat transfer.

The convective heat transfer involves the dimensionless parameters for the flow averaged over of the characteristic length L (height of the heater in this case), such as: the Prandlt number (Pr), Grashof number (Gr_L), Rayleigh number (Ra_L) and Nusselt number (Nu_L). Other parameters are very important such as the surface area and the temperature of the

heater's surface and the sink temperature of the air surrounding it. More detailed explanation of the dimensionless numbers will follow in subsequent sections.

For the channel that exists between the heater and the wall, the calorimetric approach was opted for in the evaluation of the heat transferred from the heater in that area, as a substitute to the natural convective heat transfer model applicable only to the outer surface of the heater.

The radiation heat transfer involves parameters such as:

- The absolute temperatures of the various surfaces dealt with.
- The view or shape factor (F) between the emitter (heater's surface) and sink (enclosure's) surfaces.
- The emissivity (ε) of the surfaces of the heater and the enclosure.
- The magnitude of the areas involved.

2.2 Background on the physics of the topic

Heat energy leaves the surface of the heater by two distinct modes:

i. Natural or Free convection
ii. Radiation

2.2.1 Free convection heat transfer

This section describes the energy in the form of heat that is transferred from the heater's surface to the rest of the enclosure, through the warming of the enclosure's air. It is theoretically related to the natural convection heat transferred from a vertical hot plate to a surrounding fluid.

When the heater operates, energy is transferred from its surface to the layer of fluid (air) that is immediately adjacent to this surface. The change of density of the air due to heating coupled with the generated buoyancy forces causes this heated (lighter) air to rise away from the hot surface, making room for colder (heavier) air to replace it and hence a free convection airflow is established.

This free convection flow's profile presents a velocity boundary layer that starts from the leading edge (bottom edge of the heater) and grows regularly in thickness within a given

vertical span (in the laminar zone), before becoming possibly irregular towards the exit (in the transitional and turbulent zones).

In no slip boundary condition, the velocity of flow in the laminar zone is zero at the heater's surface, increases rapidly to a peak roughly in the middle of the stream and then decreases again to zero at the outer boundary with the surrounding stationary air. The temperature however decreases regularly from the plate's surface to the surrounding or sink temperature of the air.

The flow profile described above is illustrated in Figure 2.1.
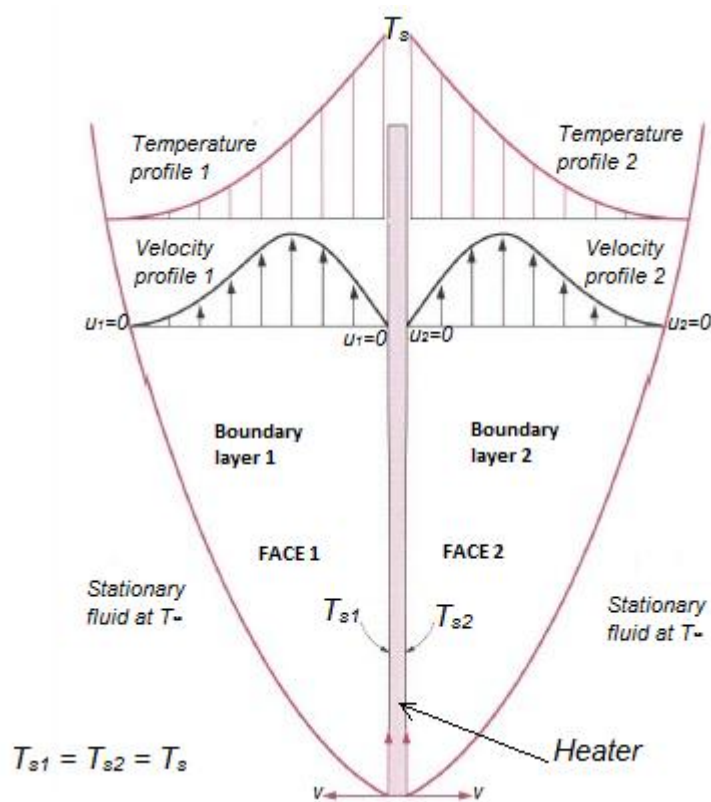
Figure 2-1:   Velocity and temperature profiles on both faces of the heated vertical plate in air

Prandtl number

It is a dimensionless parameter defined as the ratio of the hydrodynamic to the thermal boundary layer, understood as the ratio of fluid properties controlling the velocity and temperature distributions [10]. The Prandtl number [11] is expressed in Equation (2-1) as:

$$\mathrm{Pr} = \frac{v}{\alpha} = \frac{\mu C_p}{k}.$$ (2-1)

9

Given that; $\alpha = \dfrac{k}{\rho \times C_P}$ and $v = \dfrac{\mu}{\rho}$,

Where,

> Pr is the Prandtl number (dimensionless)
> v is the kinematic viscosity of air (m^2/s)
> α is the coefficient of thermal diffusivity of air (Conductivity/(density x specific heat) in m^2/s
> μ is the absolute viscosity of air (kg/(m.s)) or (Pa/s)
> C_p is the heat capacity of air at a constant pressure (J/kg/K)
> k is the coefficient of thermal conductivity of the air (W/(m.K))

Depending on the Prandtl number (Pr), the velocity boundary layer may be thinner (Pr<1) or thicker (Pr>1) than the thermal boundary layer [10]. In the instance of this study, the Prandtl number (of air) is Pr ≈ 0.71.

Grashof number

Air flowing over the hot surface of the heater's vertical surface undergoes a change in its overall properties due to heating. The rising of hot air to give way to cold air is accompanied by some shearing effects (friction) between their respective molecules, which put into evidence the interaction of the buoyancy forces with the viscous forces in the process. Figure 2.2 illustrates the description.
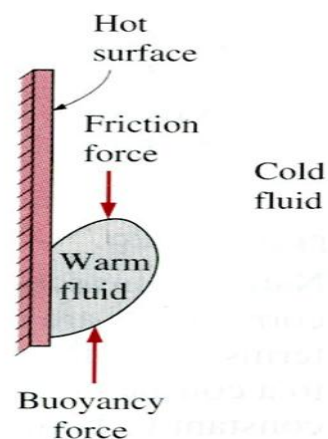
Figure 2-2:   Buoyancy and frictional forces operating on the surface of a heated vertical plate [10]

The Grashof number as described above is therefore a dimensionless parameter representing the ratio of the buoyancy force to the viscous forces in the free convection flow system [12]. The Grashof number [13] is expressed in Equation 2-2 as follows:

$$Gr_L = \rho^2 \frac{g\beta(T_S - T_\infty)L^3}{\mu^2}$$
(2-2)

where,

L is the characteristic length (height) of the heater (m)

Gr_L is the Grashof number with respect to the characteristic length of the heater (dimensionless)

g is the gravitational constant (m/s^2)

β is the coefficient of thermal expansion of the air (1/K)

T_S is the temperature of the heater's hot surface (K)

T_∞ is the room's air temperature (K)

ν is the kinematic viscosity of the air in the room (m^2/s)

Rayleigh number

It is a dimensionless number (often utilized by researchers) obtained through the product of Grashof and Prandtl numbers when formulating Natural convection phenomena [14], as expressed in Equation 2-3:

$$Ra = Function(Gr, \Pr).$$
(2-3)

Nusselt number

At the surface of the heater, the layer of air molecules adjacent to its surface is motionless. Heat transfer through the fluid layer would be by convection when the fluid involves some motion and by conduction when the fluid is motionless.

The convection heat transfer rate [15] can then be expressed as:

$$Q_y = h_L A(T_S - T_\infty)$$
(2-4)

And because the heat transfer at the surface is by conduction,

$$Q_y = -kA \frac{\partial}{\partial y}(T - T_S)\Big|_{y=0}$$
(2-5)

These two terms are equal; thus

$$-kA \frac{\partial}{\partial y}(T - T_S)\Big|_{y=0} = hA(T_S - T_\infty)$$

Rearranging gives,

11

$$\frac{h}{k} = \frac{\left.\frac{\partial (T_S - T)}{\partial y}\right|_{y=0}}{(T_S - T_\infty)}$$

Making it dimensionless by multiplying by representative length L,

Thus the Nusselt number is derived as:

$$Nu_L = \frac{hL}{k} = \frac{\left.\frac{\partial (T_S - T)}{\partial y}\right|_{y=0}}{\frac{(T_S - T_\infty)}{L}} \qquad (2\text{-}6)$$

The parameters in equations (2-4) (2-5) and (2-6) are defined as follows;

h is the coefficient of convective heat transfer W/(m^2.K)

A is the surface area of the heater (m^2)

L is the characteristic length (height) of the heater (m)

k is the coefficient of conduction of air W/(m.K)

$(T_S - T_\infty)$ is the temperature difference between the hot surface and the ambient (K)

Nu_L is the Nusselt number with respect to the heater's characteristic length (dimensionless)

There are a number of empirical equations that are applicable for the phenomenon of natural or free convection; however, the correlation below proposed by Churchill and Chu [16] applicable for a wide range of Rayleigh numbers in the laminar region will be used in this study as expressed in Equation 2-7.

$$Nu_L = 0.68 + \frac{0.67 Ra_L^{\frac{1}{4}}}{\left[1 + \left(\frac{0.492}{Pr}\right)^{\frac{9}{16}}\right]^{\frac{4}{9}}} \qquad \text{for} \qquad Ra_L < 10^9 \qquad (2\text{-}7)$$

Coefficient of convective heat transfer

An experimental process involving the application of Equation 2-7 would enable the determination of the coefficient of convective heat transfer.

Convective heat transfer from the surfaces of the heater

The rate of convective heat transfer from the vertical heater's surface can be evaluated using the following equation:

$$Q_{Conv} = h \times A(T_S - T_\infty) \qquad (2\text{-}9)$$

where,

Q_{Conv} is the total convection heat transfer from the heater's surface (s) (W).

h is the coefficient of convection heat transfer $W/(m^2.K)$

A is the total hot surface area (m^2)

$(T_S - T_\infty)$ is the temperature difference between the heater's hot surface and the ambient air. (K)

2.2.2 Radiative heat lost from the heated vertical plate

Radiation in general refers to energy emitted within the wavelength range of ($\lambda = 100nm$-$100\mu m$). However, the thermal radiation referred to in this study is made of electromagnetic waves emitted from the hot surfaces of the heater and spread over the surrounding, in the wavelength band between ($\lambda = 0.1$ and $100 \ \mu m$), (this is the band of visible radiation as well as some ultraviolet radiations) [17].

By definition, an ideal surface known as a black body, at a temperature above absolute zero,
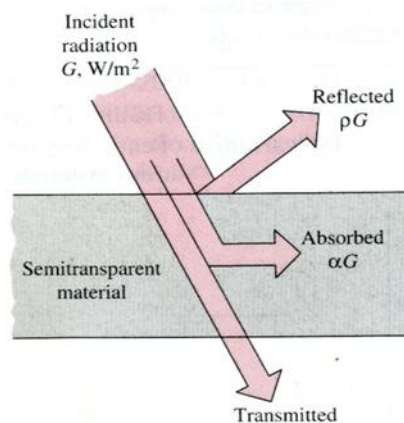
Figure 2-3:   Behaviour of incident radiation on a body. [10]

is capable of emitting a maximum amount of energy based on a surface property known as emissivity (ε) having a value of unity. Similarly, it absorbs all incident radiation because of another surface property called absorptivity (α) equal to unity as well. The above is deduced by the assumption (using Figure 2.3) that incident radiation on a black body does not reflect any portion of it neither any portion gets transmitted hence all energy gets absorbed.

13

Real bodies known as 'grey' bodies emit and interact with incoming radiation from the surrounding surfaces governed by the surface properties mentioned above (having values comprised between zero and unity), their absolute temperature raised to the fourth power, the geometry or configuration between them established through a parameter known as the shape or view factor (F) and a constant known as the Stefan-Boltzmann constant.

The net radiation heat transfer between any two grey, diffuse, opaque surfaces 1 and 2 that form an enclosure is given by:

$$Q_{12} = \frac{\sigma\left(T_1^4 - T_2^4\right)}{\dfrac{1-\varepsilon_1}{A_1\varepsilon_1} + \dfrac{1}{A_1 F_{12}} + \dfrac{1-\varepsilon_2}{A_2\varepsilon_2}} \qquad (2\text{-}10)$$

where,

σ is the Stefan-Boltzmann constant aprox. equal to: $\sigma = 5.67 \times 10^{-8}$ W m^{-2} K^{-4}

ε_1 and ε_2 are the emissivity of surfaces 1 and 2 respectively (dimensionless)

T_1 and T_2 are the absolute temperatures of surfaces 1 and 2 respectively (K)

A_1 and A_2 are surface areas 1 and 2 respectively (m^2).

F_{12} is the form or view factor between surface 1 and 2 (dimensionless)

Q_{12} is the net radiation heat transfer between surface 1 and 2 (W).

2.3   Heater mounted against the wall

As described in Chapter 1, the mounting of the heater against the wall is a phenomenon on its own when compared to similar space heaters standing free in an arbitrary floor position within an enclosure.

The behaviour or mechanism of heat transfer from the heated vertical plate facing the wall on which it is mounted and hence creating a channel is quite ambiguous. If a boundary layer flow exists on the heater's inner surface facing the wall, the heat transfer by natural convection may be predicted through the use of empirical formulae obtained or available from the literature. Concentrated or focussed perusal of the literature did not yield any results pertaining to the particular geometry being investigated in this work. The closest encountered published work is for a channel formed by two vertical parallel hot plates. For example:

Two boundary layers of flow are predicted for a vertical channel made by two isothermal walls symmetrically heated [10], while numerical investigations are provided in the study of

the heat transfer on vertical plates placed in V-position instead of purely vertical parallel positions and the vertical plates with wavy surfaces. [18]. Geometry tests (variation of height from the floor and gap space from the wall) were also performed for a vertical plate with the surface of the plate facing the wall insulated [19]; attempt to match the results with those obtained through a simulation using ANSYS (a finite elements software package), showed an increase in the heat transfer coefficient from the heated surface of the plate when the height with respect to the floor was smaller than the gap space from the wall.

In the present study, the global behaviour of heat transfer through the vertical channel gap formed by the heater's inner surface and the wall that it is mounted on, will be dealt firstly with existing empirical formulae that assume the existence of a classical boundary layer. In the event of disagreement on the heat balance on the heater by the sum of convective and radiative heat losses with the electrical energy input, a calorimetric approach [20] for the measurement of heat through the channel will be adopted. This will entail determining the amount of heat gained by the air stream whilst flowing through the channel, given by the relationship:

$$\dot{Q}_{Cal} = \dot{m} \, Cp_{inlet} \left(T_{outlet} - T_{inlet} \right) \tag{2-11}$$

and

$$\dot{m} = \rho_{inlet} \times v_{inlet} \times A_C \tag{2-12}$$

where,

$\dot{Q}_{Cal}$ is the calorimetric HT through the channel (W).

A_C is the cross sectional area of the channel (m^2)

Cp_{inlet} is the specific heat capacity of air J/kg/K

ρ_{inlet} is the density of air at the inlet (bottom) of the channel (kg/m^3)

v_{inlet} is the velocity of air at the inlet (bottom) of the channel (m/s)

$\dot{m}$ is the mass flow rate of air going through the channel (kg/s)

$T_{outlet} - T_{inlet}$ is the temperature difference between the hot air exiting the channel and the fresh air entering it. (K)

2.4   Summary

In this chapter, an attempt was made to present an overview of the theoretical background on convective and net radiative heat transfer modes from the geometry created by mounting a heater (conforming to a vertical heated surface), against an enclosure's wall. The literature survey presented fundamental equations as well as choices of various empirical equations. These tools will be used when attempting to evaluate the heater's performance through parametric studies involving the mounting geometry relative to the enclosure. The next chapter will endeavour to cover the experimental protocol that was adopted in this study.

CHAPTER 3

RESEARCH METHODOLOGY

3.1   Introduction

The theoretical background related to the physics of a heated vertical plate in air, was presented in the previous chapter; what follows here is the description of the mounting assembly, measuring devices as well as the experimentation protocol of the various tests that were undertaken using the 'commercial' donated wall-mounted heaters.

3.2   Mounting assembly

The description of the mounting assembly highlights the initial design and manufacturing of some of the external supports or framing components for the heater. The configuration of the various components for each specific experiment together with its experimental procedure, occupy a major portion of this chapter. The mounting assembly is made of the following respective groups of components (heaters, mounting and insulating kits) that were assembled as shown in Figure 3.1.
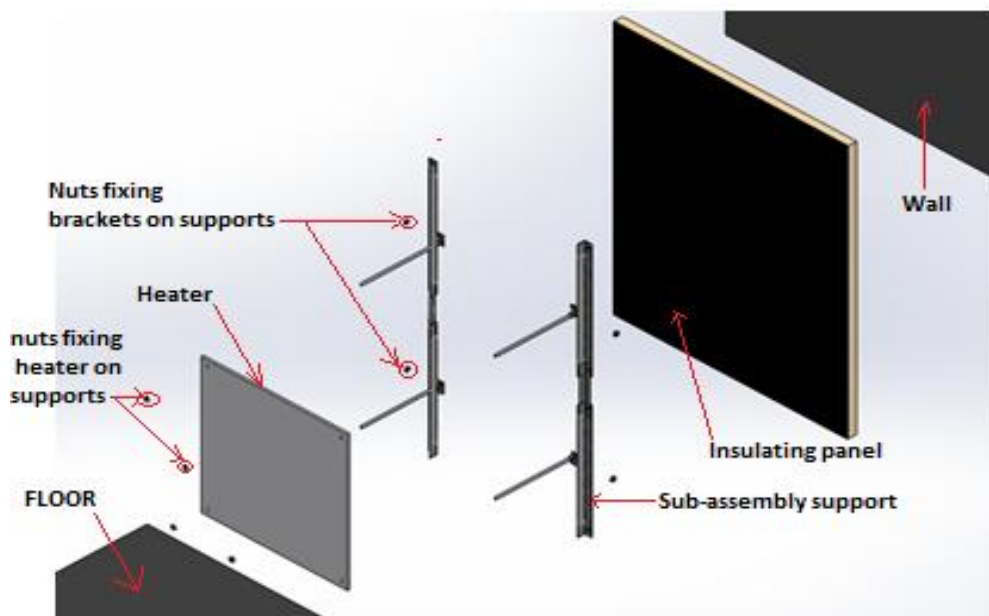
Figure 3-1:   Exploded view of the wall mounted space comfort heater

3.2.1 **Heaters for the tests**

Two identical heaters with the specifications shown in Table 3.1; were graciously offered by the manufacturer for the experiments.

Table 3-1:   Heater's specifications

Power Rating:	1.7Amps @ 230V 50 Hz
Measured Resistance	127 Ω ohms
Overall Dimensions	~ 600 x 600 x 10mm
Max Surface Temp.	Approx. 75 – 90° C, depending on the ambient temperature
Mass	6kg
Plug	3 point, not earthed (world market: depending on country specs)
Approx. Quantities:	1 heater per 12m² floor area (temperate climate)
	1 heater per 8m² floor area (cold climate)

3.2.2 **Mounting kit**

It was designed and manufactured as a set of components comprising:

- The mounting columns which were fixed against the wall to support the heater and enable vertical adjustments of positions relative to the floor (travel from 0 to 300mm).
- The brackets supporting the heater from each of its four respective corners and fixed on the above support columns.
- The collars (rings) that enabled the gap's spacing adjustments (created between wall and heater).

The assembly of the Mounting Kit is represented in the schematic diagram in Figure 3.2.
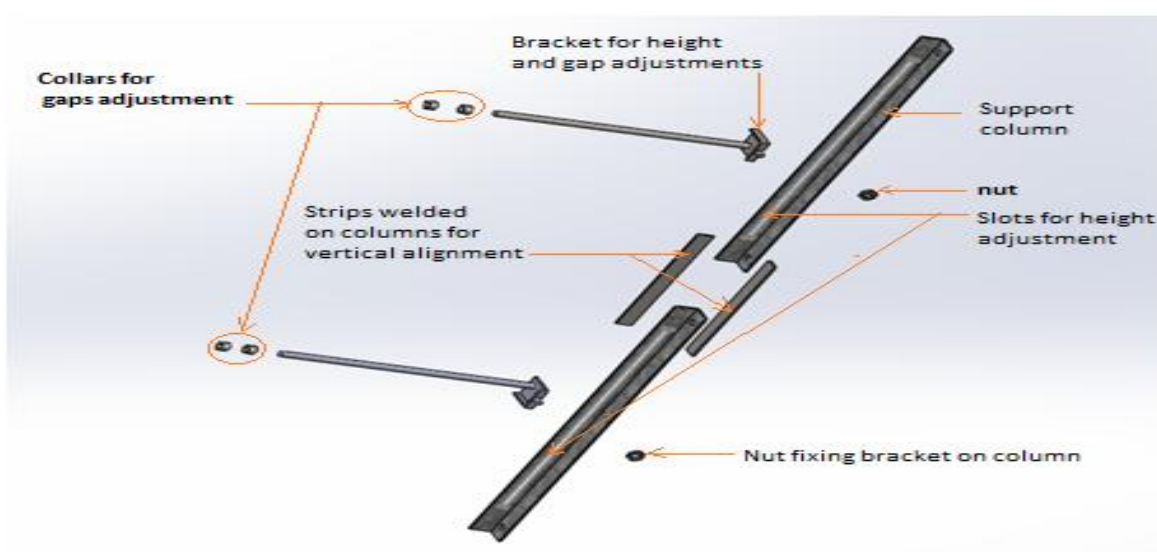
Figure 3-2:   Exploded view of the mounting kit

3.2.3 **Insulating kit**

It was a 940mm wide by 1105mm high frame made of 35mm x 35 mm square section of wood (dry pine) as depicted in Figure 3.3. This frame was screwed on the wall, filled with polystyrene pads and covered with a 3mm thick sheet of Perspex with its external surface covered with a mat black paint. The panel when assembled formed the insulation on the wall opposite the heater. The mounting kit was mounted on the insulation panel when the respective tests were performed.

Figure 3-3:   Insulating panel

3.3 **Measuring devices**

The following devices and components were interconnected with each other into a well-structured sequence to form the measuring system or instrumentation linking all the hot sources to be investigated (input) to a final reading device (output), for the recording of data of the various experiments:

3.3.1 **Multimeter**

The Fluke 8050A digital multimeter in Figure 3.4 with resolution up to centimes was used for measuring the thermocouples' output in millivolts, which were later converted into degrees centigrade, with the use of conversion tables and double-checked with online converters.

All the data of the various tests were recorded manually from the multimeter and stored in spreadsheets for further analysis, because the multimeter via its connection to the switchboard offered a wide range of readings at a time.

Figure 3-4:   The Fluke 8050A Digital multimeter

3.3.2   **Thermocouples**

Figure 3.5 depicts the used chrome-alumel thermocouples, known as K-type. Their inputs (the beads) were attached onto the required surfaces and their outputs to selector switches connected to the millivolt output setting of the measuring device (the multimeter).
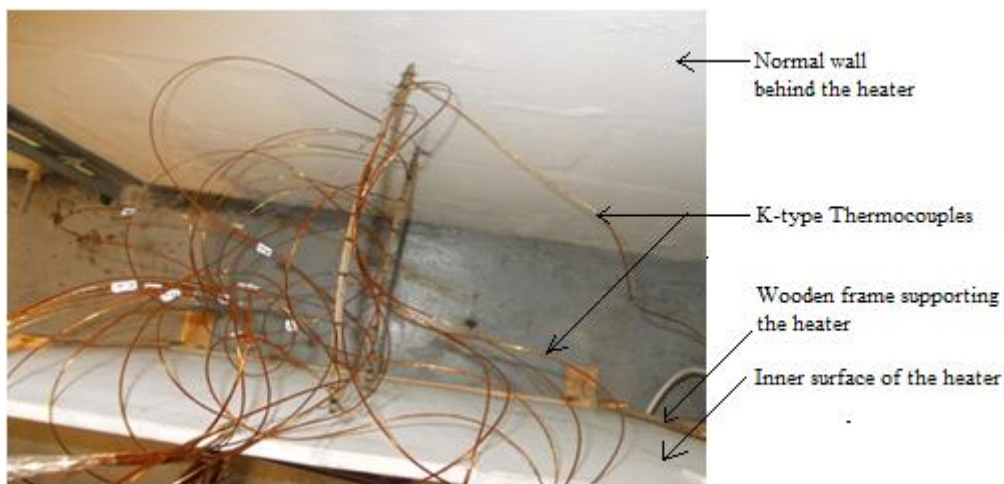
Figure 3-5:   Chromel-alumel (K-types) thermocouples

3.3.3   **The switch system**

Two-poles-six-ways rotary switches of type Alpha RSW 2P 6W SL40, (a total of seven

(a)   (b)

Figure 3-6:   Switch system: (a) Switch-board, (b) two pole-six position rotary

20

switches which were later reduced to 4), were connected to connectors and thermocouples to form the switch system as shown in Figure 3.6. The output from each thermocouple was soldered on the specific input ports of the switch. The output position of each rotary switch was selected in turn and connected to the multimeter to measure the readings in millivolts.

3.3.4 Data-logger

Shown in Figure 3.7 is the EL-USB-TC type Data-logger (Easylog USB) that was mostly used at the calibration phase because of its single thermocouple-reading at a time, to check the accuracy of the other measuring device (Fluke) (see 3.3.1). To use it, a single thermocouple ends initially fixed on a switchboard connected to the Fluke were removed after their reading was taken from the Fluke, and fixed on the plug (green in the picture) that was in turn plugged into the socket end of the data-logger. The USB output end of the data-logger was then plugged into a laptop computer; sothat the data could be outputted graphically (or numerically when necessary) on the laptop's monitor so to confirm the reading of the Fluke. The data-logger is suitable for a -200°C to +1350°C temperature range, ideal for K-type thermocouples. Its accuracy is +/-1°C.
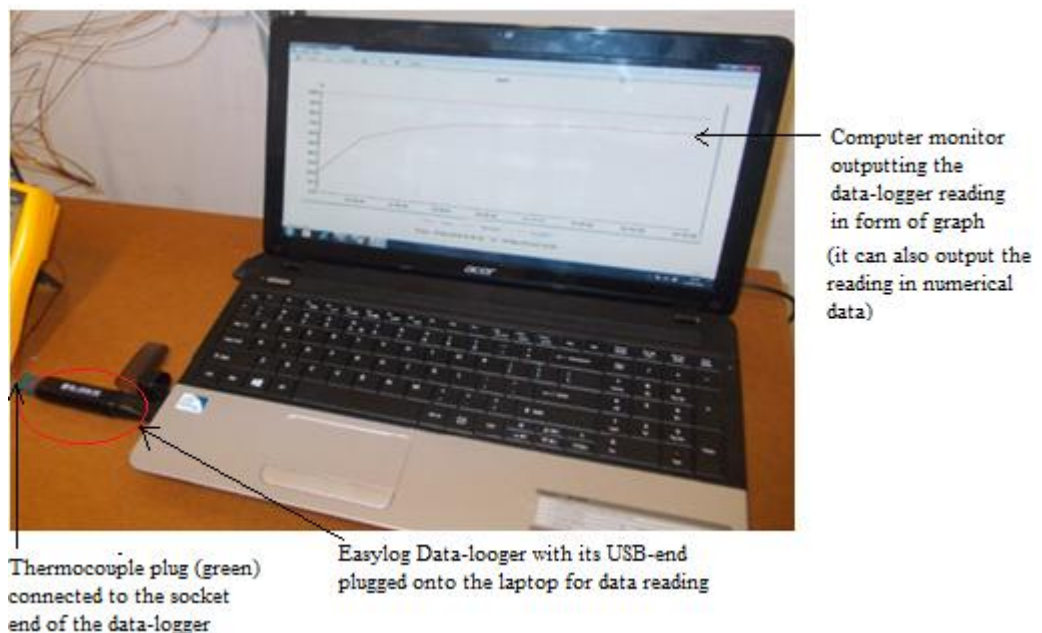
Figure 3-7:   An EL-USB-TC Data-logger plugged onto the computer: its output on monitor

3.3.5   Digital clamp meter

Shown in Figure 3.8 above is a digital clamp meter of type M266 that was set to 200A range with a resolution of 0.1A, to measure the AC current input to the heater.
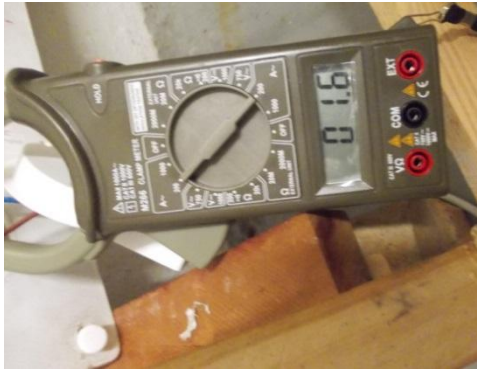
Figure 3-8:   M266-type digital clamp meter

3.3.6 **Infrared gun**

The infrared device used is a Minolta / Land Cycleps Minilaser, (max 1.0 mW, 650 nm), portrayed in Figure 3.9. It was utilised mostly to check the emissivity of various heated surfaces on test.

Figure 3-9:   Minolta/Land Cycleps Minilaser

3.3.7   **Velocimeter**

Figure 3.10 depicts models of: (a) Mechanical air velocity meter with impeller and (b) electronic air velocity meter with probe [21], that were used to measure the velocity and the temperature of hot air leaving the channel created by the heater and the wall it was mounted on. The digital velocimeter 9535 more accurate was used for most of the tests through the channel. Its accuracy is defined as follows:

In velocity: $\pm 3\%$ of reading for the range of 0-30m/s (0-600ft/min)   ,   meaning $\pm 0.015 m/s \left(\pm 3 ft/\min\right)$, whichever is greater.

In temperature: $\pm 0.3^{o} C \left(\pm 0.15^{o} F\right)$ for the rage -18 to 93°C (0 to 200°F).[22]
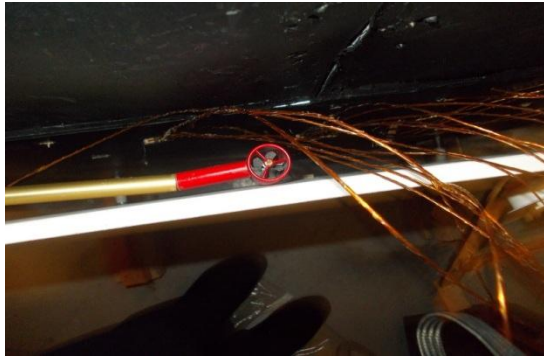
(a)   (b)

Figure 3-10:   Velocimeters (a) Mechanical with impeller (b) Velocimeter 9535 with probe

3.3.8   **Table of temperature conversion**

Table of temperature conversion as shown in Appendix B was utilised to convert millivolt recorded temperatures into degrees Celsius.

3.3.9   **Online temperature converter from mV to °C**

Figure 3-11: Flukes online temperature converter from millivolt to degree Celsius

23

Figure 3.11 depicts the online calculator [23] utilised to double-check the converted temperatures mentioned in Section 3.3.8.

3.3.10 Miscellaneous items

Aluminium foil and black mat paint were alternatively used besides the normal grey wall, to change the wall conditions behind the heater inside the channel. Super-glue was used to attach the thermocouples on the surfaces. Rulers and tape-measuring band were also used for height and gap measurements and finally some fasteners were used for the fixation of the overall system.

3.4 Experimentation protocol

It describes preliminary conditions for all the tests and the effects of running these tests. The work involved in this section was accomplished in two phases:

- Phase I: The calibration of all the measuring devices
- Phase II: The experimental protocol

3.4.1 PHASE I: Checking of measuring devices (calibration) and results

All measuring devices used in the various experiments were subjected to a checking process so to ensure that they fulfilled the requirements of precision and accuracy and that their respective specifications also conformed to international standards.

Calibration of the room's air temperature thermometers

The thermometers used for the measurement of the room temperature were designed for a temperature range between -10°C to 150°C. They were calibrated in boiling water and in ice-water slush. Care was taken to prevent the thermometers from contacting the container being used, as this could result in erroneous temperature reading. Figure 3.12 depicts one of these thermometers*.*

They were six simultaneously used and were the Red-alcohol-filled thermometers, model L0132/10 measuring 305mm long, with divisions of 1.0 unit [24], full immersion type. They were hung at six different positions randomly chosen inside the enclosure where the experiments were conducted.

The thermometers used for the measurement of the room temperature were designed for a temperature range between -10°C to 150°C. They were calibrated in boiling water and in ice-

water slush. Care was taken to prevent the thermometers from contacting the container being used, as this could result in erroneous temperature reading. Figure 3.12 depicts one of these thermometers.

They were six simultaneously used and were the Red-alcohol-filled thermometers, model L0132/10 measuring 305mm long, with divisions of 1.0 unit [24], full immersion type. They were hung at six different positions randomly chosen inside the enclosure where the experiments were conducted.

The thermometers used for the measurement of the room temperature were designed for a temperature range between -10°C to 150°C. They were calibrated in boiling water and in ice-water slush. Care was taken to prevent the thermometers from contacting the container being used, as this could result in erroneous temperature reading. Figure 3.12 depicts one of these thermometers.

They were six simultaneously used and were the Red-alcohol-filled thermometers, model L0132/10 measuring 305mm long, with divisions of 1.0 unit [24], full immersion type. They were hung at six different positions randomly chosen inside the enclosure where the experiments were conducted.

The thermometers used for the measurement of the room temperature were designed for a temperature range between -10°C to 150°C. They were calibrated in boiling water and in ice-water slush. Care was taken to prevent the thermometers from contacting the container being used, as this could result in erroneous temperature reading. Figure 3.12 depicts one of these thermometers.

They were six simultaneously used and were the Red-alcohol-filled thermometers, model L0132/10 measuring 305mm long, with divisions of 1.0 unit [24], full immersion type. They were hung at six different positions randomly chosen inside the enclosure where the experiments were conducted.

The thermometers used for the measurement of the room temperature were designed for a temperature range between -10°C to 150°C. They were calibrated in boiling water and in ice-water slush. Care was taken to prevent the thermometers from contacting the container being used, as this could result in erroneous temperature reading. Figure 3.12 depicts one of these thermometers.

They were six simultaneously used and were the Red-alcohol-filled thermometers, model L0132/10 measuring 305mm long, with divisions of 1.0 unit [24], full immersion type. They

were hung at six different positions randomly chosen inside the enclosure where the experiments were conducted.

Figure 3-12: Red-alcohol filled thermometer used for the room's air temperature measurement

Checking the multimeter and data-logger

The six thermometers were hung inside the tests' enclosure with a thermocouple alongside each.

The readings of each thermocouple measured with the multimeter and converted into temperatures, confirmed the corresponding readings on the thermometer adjacent to them.

Similar tests were performed using the data-logger. Another connection was made from the same hot source to the laptop's monitor through a thermocouple and data-logger. The outcomes of these tests on the laptop's monitor substantiated the temperature readings from the thermometer.

Checking the heaters

The two heaters for the experiments were pre-checked in terms of dimensions, power input and emissivity. The actual heaters dimensions measured were 588mm x 588mm x 10mm.

The actual input current and power of the two identical heaters were measured with the clamp meter, each rated at 1.7A and 391W respectively.

The emissivity measurements in terms of temperatures at various points adjacent to the fixation points of the thermocouples on the heater's surface with the infrared gun were as follows:

- The temperature at a marked point on the heater's surface was recorded.
- The laser from the infrared gun was aimed on this point to enable the measurement of the temperature. By adjusting the emissivity value in the infrared gun, the temperature reading was matched to the thermocouple reading and hence the emissivity of the surface was established.

This process was repeated at various points of the enclosure's walls exhibiting an average emissivity value of 0.76.

Calibration of the thermocouples

A switch-board made of 7 identical two-pole-six-positions switches to create a total of 42 thermocouples, were connected to the multimeter. At first, the thermocouples were placed into a container of distilled watery ice slush. Readings were recorded for each thermocouple and an overall maximum variation of plus or minus 0.02mV corresponding to the range of temperature between -0.5^{o}C and +0.5^{o}C was deemed acceptable.

Subsequently, the thermocouples were immersed into distilled boiling water and measurements in the range of 4.06 mV to 4.14 mV, corresponding to 99°C to 101°C were recorded.

Emissivity of: Black wall, black panel and aluminium foil surfaces

The emissivity of all these surfaces was checked using the infrared gun as mentioned previously and following the same protocol as in Section 3.4.1.3. It was established that for the black wall as well as black panel, the value of the emissivity was 0.99 and 0.05 for the aluminium foil covered surface.

Room's air temperature

The temperature of the air in the enclosure was always measured before, during and after the various tests with the hanging thermometers and confirmed with the probe of the digital thermocouple / velocimeter. During all the experiments conducted, the room's air

temperature did not vary with time more than 1°C because of the non-hermetical state of the enclosure.

All the tests were performed as described in the testing protocol detailed in Phase II which follows.

3.4.2 Phase II: Testing / Experimentation protocol

Table 3-2:   List of experiments performed

Experiment	Description
1	Heater's performance when freely positioned inside the enclosure (far from any wall)
2	Heater's performance when mounted at various gaps from the wall.
3	Heater's performance when mounted at various heights from the floor
4	Heater's performance affected by surface conditions of the wall where it is mounted (i.e. low emissivity, high emissivity and high emissivity insulated wall).

The various experiments performed to determine the space heater's performances were carried out in the sequence shown in Table 3.2.

Experiment no.1: Heater's performance when freely positioned inside the enclosure (far from any wall)

The heater was freely positioned inside the enclosure far from any wall. It was mounted on a wooden stand at a height of 250mm above the floor. This test aimed to obtain/establish the performance of the heater with view to be used as a benchmark with regards to its overall efficiency for all the tests conducted

i)   The system was primarily assembled and calibrated in-situ.

ii) Thermocouples were glued on respective measuring points on the heater's surfaces

iii) The room's air temperature was recorded

iv) The heater was turned on and data were only recorded when steady state was achieved (at least 45 minutes from starting) as shown in Figure 3.13. The steady state here is the operational condition in which temperatures at respective surfaces as well as of flows remain constant. At this point, displays of the multimeter and of the data logger stopped fluctuating / rising.

v)   The input current and voltage to the heater were recorded.

vi) Temperatures were recorded and stored on the spreadsheet in millivolts (mV) for each individual point of measurement on the heater's surface.

vii) Convection and radiation heat transfer were evaluated from the recorded data**.**
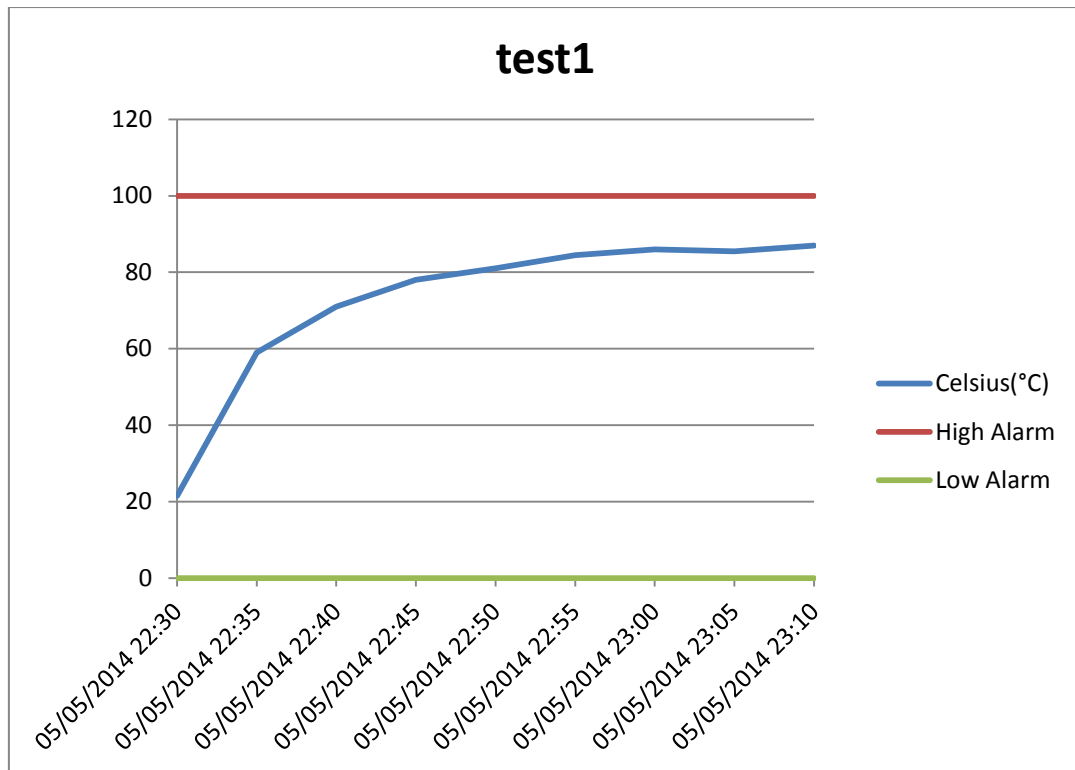
Figure 3-13: Data-logger's graph for the temperature on the heater's surface from start-up to steady-state

The evaluation of the convection heat transfer from the heater surfaces required the following steps:

i)   All individual mV recorded temperatures were converted into °C.

ii) The average temperature of the heater's surfaces facing the walls of the enclosure was determined (T_{outer}), followed by the subsequent film temperature.

iii) Properties of air were determined at film temperature from a table and with the use of the converter (see Figure 3.11). For details, refer to Table 6.1 in Appendix A.

iv) The Grashof Number was determined with the use of Equation (2-2).

v) The Rayleigh Number was determined through Equation (2-3).

vi) The Nusselt Number was evaluated with the use of Equation (2-7).

vii) The coefficient of convective heat transfer *h* was obtained from the Nusselt number

viii)   The total convection heat transfer from the heater's surface was evaluated using Equation (2-9).

The net radiation loss from the heater's surfaces was determined using Equation (2-10) applied between the heater and the enclosure's walls.

After this benchmarking test, all other experiments were conducted with the heater mounted against the wall.

Experiment no.2: Heater's performance when mounted at various gaps from the wall

These were the tests conducted at various gaps that were created between the heater and the wall, with its height from the floor kept constant within the range recommended by the manufacturer. The heater was mounted utilising the mounting kit at a height of 250mm from the floor. Gaps were varied from 10mm to 300mm. Measurements of temperature for each individual point on the heater's surface, the wall behind the heater; the air temperature in the room and the temperature of the walls of the room were made. In addition, the emissivity of each surface (the enclosure's walls and heater's surface) was determined with the Infrared Gun.

 The calorimetric procedure to establish the gap's contribution to warming the enclosure's air

Tests were initially performed assuming the environment's air behaviour to be the same as in the normal free stream in a room. The wall behind the heater as well as the heater's surface facing this wall were considered to be receiving a natural stream of ambient air all along the heater's characteristic length; hence, the use of the classical free convection equations could be applied for the determination of the free convection coefficient. This initial approach to establish the heater's performance bore results out of range with the overall heat balance exceeding sometimes the electrical input into the appliance.

It was therefore assumed that the ambient air was impeded / restricted in entering the channel that existed between heater and wall. The air in the channel was unlikely to have a free entrainment of ambient air along the "hot air boundary layers" of either on the wall side or on the inner surface of the heater.

The wall side of the channel could contribute in warming up the air as well. The wall could receive energy by convection as well, but mainly by radiation from the heater's surface and although it should lose heat by conduction through the wall, there remained enough energy to elevate its temperature above the ambient air temperature as well as the other walls of the room. It is suggested here that the wall also contributes by some means to the final temperature rise of the air from the inlet to the channel's outlet. Studies that deal with natural convection flow in a vertical open-ended channel with wall constant heat flux have been reported in the literature; however, the author is unaware of any analytical or empirical formulation and solution of a heat transfer problem which caters for the geometry encountered in this project.

As a palliative to the situation, the calorimetric approach was used for the evaluation of the net heat delivered by the air from the channel. This approach was henceforth to be used for all the experiments of the wall mounted heater.

The procedure consisted of measuring the amount of hot air exiting the channel. The mass flow rate of air was arrived at by the measured velocities as well as temperatures with the velocimeter and the calorimetric relationship was applied to the evaluation of the heat flow.

The final steps (in detail) performed for all the tests conducted on the heater mounted against the wall, were, as described below, the followings:

- The average temperature of air was determined at the inlet (bottom) of the channel (T_{inlet}).
- Properties (density (ρ_{in}) and specific heat capacity ($C_{p_{in}}$)) of fresh air entering the channel and almost similar to the room temperature were determined from a table of properties of air.
- Velocity of air (v_{in}) was measured at the inlet of the channel with the velocimeter and a thermal air probe respectively.
- The average temperature of hot air was determined at the outlet (top) of the channel (T_{outlet}).
- Temperature differences across the Channel were determined (for the respective gaps) using the relationship: $\Delta T_{Chan} = T_{outlet} - T_{inlet}$.
- Cross sectional Areas were evaluated for each respective gap: A = Gap size x width of Heater.
- The mass flow rate of air through the channel was evaluated through Equation (2-12).
- The calorimetric Heat therefore being delivered to the enclosure was evaluated by the use of Equation (2-11).

NB: The "calorimetric" heat transfer is just a component of the total heat transfer in all the experiments of the heater when it is mounted on the wall.

Investigation of the temperature distribution across the channel

Average temperatures were measured across the channel gap from the heater surface to the wall facing it. The study was conducted with the heater mounted at a geometry conforming to

the range of the heater's optimal performance determined from Section 3.4.2.2. The aim was mainly to investigate the temperature behaviour across the channel gap between the heater and the wall. The heater was mounted at a height of 250mm above the floor and a gap of 50mm from the wall.

Experiment no.3: Heater positioned at various heights from the floor

These were the tests conducted at various heater's heights from the floor (which included the manufacturer's recommendation), at a gap conforming with a range that provides an optimal performance to the heater. The heater was mounted on the normal grey wall at a gap of 50mm from the wall, using the designed mounting kit. The heights were varied from 0 to 300mm.

Experiment no.4: Heater mounted facing "walls" of low emissivity, high emissivity, and insulated wall with high emissivity

The wall behind the heater was made successively shiny (low emissivity), painted mat black (high emissivity) and lastly, an insulated panel with its surface painted mat black (high emissivity) that was fixed on the wall, prior to the mounting of the heater in each scenario. The heater was mounted at a height of 250mm from floor and a gap of 50mm from wall. The aim of these experiments were to examine the effects of the reflective surface, the high emissivity and the insulation of the wall with regard to the heat transferred by the air passing through the channel and contributing to the heating of the enclosure.

3.5 Summary

In this chapter, a description of the methodology in carrying out the tests on the wall mounted space comfort heater was presented. Data recorded during the tests were to be analysed with view of determining to what extent the various parameters affected the performance of the heater. The analysis of all data is detailed in the following chapter.

CHAPTER 4

RESULTS AND DISCUSSIONS

4.1   Introduction

The fulfilment of all sequences of the experimentation described in Chapter 3 implied the tests performed on the heater, which culminated in the recording of their outcomes or data. The data were subjected to various analyses that could enable a better understanding of the heater's performance.

The performance of the wall mounted heater is based on the total heat transferred from the heater to the air of the enclosure for each respective mounting condition. In terms of the heater's efficiency, it was based on the total convective heat transferred from the heater to the air of the enclosure vis-à-vis the total electrical energy input.

The experiments were conducted at a room temperature of 24 °C with a variation not exceeding +/-2 °C.

4.2   Experiment no. 1 - Heater freely positioned inside the enclosure

Temperatures were recorded on the spreadsheet in mV and in °C, as described in Chapter 3. The average temperatures along the heater's characteristic length for both surfaces were around 80°C, with relatively lower values at the bottom part and higher values at the upper part. The range of variation of the heater's surface temperature along the height was +/-5°C. Data recorded for the experiment with the heater standing freely in the middle of the enclosure are presented in Table 4-1.

Table 4-1:   Temperature (in mV and in °C of the heater's surfaces when freely mounted

Face 1)		Face 2	
mV	°C	mV	°C
2.41	82.36	2.42	82.6
2.37	81.4	2.37	81.4
2.31	79.95	2.29	79.59
2.21	77.55	2.22	77.79
2.12	75.5	2.12	75.38
Average	79.35	Average	79.35

These data were processed for the evaluation of heat transfer from both surfaces of the heater when it was freely mounted inside the enclosure.

The heater's performance determined from the HT analysis resulting from the above temperatures in the present mounting condition, is presented in Table 4-2

Table 4-2:   Results of the heater's experiment no. 1 (standing freely inside the enclosure)

Heater surfaces	Tout °C	T-film °C	ρ kg/m^3	Cp kJ/kg.K	k W/(m.K)	v x 10^{-6} (m^2/s)	β x 10^{-3}(1/K)	Pr	Gr	Ra=Gr*Pr	NuL	h W/(m^2.K)	Qout (W)	rad_o (W)	Q$_{Total}$ (W)
face 1	79.35	51.68	1.09	1.01	0.03	18.14	3.08	0.72	1.17E+09	8.48E+08	88.6	4.14	79.2	113.7	192.9
face 2	79.35	51.68	1.09	1.01	0.03	18.14	3.08	0.72	1.17E+09	8.48E+08	88.6	4.14	79.2	113.7	192.9
Total													158.5	227.4	385.9

The efficiency (as defined under 4.1) of the space heater in this scenario was:

$$\eta_{conv} = \frac{Q_{conv}}{Q_{IN}} \times 100 = \frac{158.5}{391} \times 100 = 41\%$$

Where Q_{IN} is the measured electrical energy and Q_{conv} the total energy transferred to the enclosure's space.

4.3   Heater mounted on the wall

When the heater was mounted on the wall, a considerable increase of temperature was recorded on both of its surfaces compared to when standing in the middle of the enclosure, with the inner surface (facing the wall) being slightly hotter than the outer surface (facing the rest of the enclosure). This effect became increasingly acute with an average increase around 25% and 20% at the inner and outer surfaces respectively depending on the narrowness of the gap in the channel.

The increase of the heater's inner surface temperature could be justified by the conjugate effect of air warmed by convection and dwelling inside the narrow channel and by the lesser net radiation heat transfer loss from the heater's inner surface, since the wall where the heater was mounted was at higher temperature compared to the rest of the enclosure's walls. The increase in the heater's outer surface temperature resulted from the increase in its inner surface temperature that possibly manifested conduction heat transfer across the heater's body thickness.

The above described temperature increments, resulted into a performance drop of almost 60% from the heater's inner surface co-forming the channel, and a heat transfer improvement of less than 30% at the heater's outer surface facing the rest of the enclosure. Consequently, the mounting of the heater on the wall resulted into an overall sacrifice (loss) of almost 20% of

its overall performance compared to when operating in the middle of the enclosure. The temperature increase at the heater's inner surface and at the wall, possibly built up a duality that although it helped in minimising the net radiation loss from the heater's inner surface more likely affected negatively the amount of heat transferred to the mass of air that flowed through the channel.

4.3.1 Experiment no. 2: Heater's performance mounted at various gaps from the wall.

Table 4-3: Temperatures recorded in mV and converted in °C when mounted on normal grey wall

Gaps size (mm)	Normal Wall Temperatures (mV)			Gap Size(mm)	Normal Wall Temperature in °C		
	Wall	Inner	Outer		Wall	Inner	Outer
10	1.44	3.47	3.14	10	59.0	108.0	100.2
	1.28	3.37	3.02		55.1	105.7	97.1
	1.2	3.27	2.95		53.2	103.2	95.6
	1.16	3.1	2.92		52.3	98.0	94.7
	1.09	3.0	2.8		50.6	95.6	92.0
				Average	54.0	102.1	95.9
20	1.37	3.39	3.03	20	57.3	103.1	97.4
	1.19	3.24	3		53.0	102.5	96.6
	1.1	3.21	2.97		51.0	101.8	96.0
	1.04	3.2	2.95		49.5	101.5	95.5
	0.92	2.79	2.77		46.6	94.6	91.2
				Average	51.5	100.7	95.3
30	1.18	3.18	3.02	30	52.8	101.1	97.2
	1.05	3.12	2.95		49.7	99.6	95.4
	0.94	3.08	2.83		46.9	98.6	94.5
	0.9	3.04	2.78		46.1	97.6	92.5
	0.78	2.88	2.91		43.1	93.8	91.4
				Average	47.7	98.2	94.2
40	1.16	3.18	2.98	40	52.3	101.0	96.2
	0.98	3.15	2.9		48.0	100.4	94.2
	0.94	3.09	2.88		46.9	98.8	93.8
	0.88	2.96	2.87		45.5	95.8	93.5
	0.82	2.85	2.82		44.1	93.1	92.3
				Average	47.4	97.8	94.0
50	1.15	3.09	2.95	50	52.0	98.8	95.4
	0.99	3.06	2.91		48.2	98.1	94.5
	0.93	3.04	2.87		46.8	97.7	93.6
	0.9	3.01	2.83		45.9	96.9	92.5
	0.82	2.76	2.76		44.0	90.8	90.8
				Average	47.4	96.5	93.4
60	0.99	3.05	2.94	60	48.3	97.8	95.3
	0.98	3.01	2.9		47.9	96.9	94.2
	0.93	2.99	2.84		46.8	96.5	92.8
	0.92	2.96	2.79		46.5	95.8	91.7
	0.87	2.94	2.74		45.4	95.2	90.5
				Average	47.0	96.4	92.9

Mounted against the normal grey wall, the performance analysis was in this gap's variation. However, emphases were brought on two specific points during the process, one on the gap of 20 mm (as recommended by the manufacturer) and the other on the study of the

temperature profile created in the gap. For all the tests conducted during experiment no. 2, the heater was mounted against the normal grey wall at a height of 250 mm from the floor.

Evaluation of the heater's performance at various gaps from the wall.

Temperatures recorded on the heater's surfaces and the wall are presented in Table 4-3

The total heat transferred to the airflow through the channel was evaluated via the two alternative approaches emphasized:

Under the assumption of two boundary layers of flow through the channel (at the heater's inner surface and at the wall facing it), calculations were performed using the classical equations for the evaluation of all the theoretical components of heat transfer from the respective compartments of operation. Table 4-4 presents the outcome of the process.

Table 4-4:   HT results assuming boundary layers on the heater's two surfaces and the wall

	Heat transfer performance assuming boundary layers of flow on the heater's two surfaces and on the wall												
Gap size	T_{inner}	T_{wall}	T_{outer}	Pr	Gr	Ra_L	Nu_L	h	Q_{outer}	$Q_{rad-outer}$	Q_{wall}	Q_{Cal}	$Q_{rad-chan}$	Qtotal
mm	°C	°C	°C					W/(m².k)	W	W	W	W	W	W
10	102.1	54.0	95.93	0.72	1E+09	8.6E+08	89	4.25	105.6	160	36.2	116.8	100.6	519.2
20	100.7	51.5	95.34	0.72	1E+09	8.6E+08	88.9	4.24	104.6	158.3	32.5	114.2	101.2	510.8
30	98.2	47.7	94.2	0.72	1E+09	8.5E+08	88.7	4.23	102.6	154.9	27	109.6	101.1	495.2
40	97.8	47.4	94	0.72	1E+09	8.5E+08	88.7	4.22	102.2	154.3	26.6	109	100.7	492.8
50	96.5	47.4	93.42	0.72	1E+09	8.5E+08	88.6	4.22	101.2	152.6	26.6	106.6	97.4	484.3
60	96.4	47.0	92.93	0.72	1E+09	8.4E+08	88.5	4.21	100.3	151.2	26	106.5	98	482

The Results displayed in Table 4-4 are noticeably out of range, with the total heat transferred from the heater's surfaces exceeding the total electrical input (391W) to the heater. This result reveals that the initial assumption of boundary layers of heat flow from the heater's surfaces (inner surface plus wall forming the channel and outer surface), was not appropriate.

The calorimetric approach was therefore applied, as palliative to the above results, for the evaluation of the heat transfer contribution from the channel to the total received by the enclosure's air.

For the purpose of the channel's heat transfer evaluation through the calorimetric approach, the velocity of the air measured at the inlet (bottom entry) of the channel as well as the air temperatures measured both at the inlet and at the outlet (top / exit) of the channel. Their recorded and subsequent average values are displayed in Table 4-5, Tables 4-6 and 4-7 respectively.

Table 4-5:   Velocity of air at the entry of the channel with the heater mounted on normal grey wall

Gap Size (mm)	Velocity of air at the entry of the channel (m/s)					Average velocity (m/s)
10	0.15	0.17	0.17	0.16	0.15	0.16
20	0.27	0.28	0.3	0.29	0.28	0.28
30	0.29	0.29	0.3	0.31	0.28	0.29
40	0.24	0.22	0.23	0.24	0.19	0.24
	0.26	0.28	0.28	0.25	0.25	
50	0.15	0.15	0.16	0.16	0.14	0.16
	0.15	0.2	0.18	0.16	0.15	
60	0.13	0.14	0.15	0.15	0.14	0.15
	0.15	0.16	0.17	0.16	0.15	

Table 4-6:   Temperatures of the air at the entry of the channel with the heater mounted on normal grey wall

Gap Size (mm)	Temperatures at the entry of the Channel (°C)					Average temperature (°C)
10	24.8	25	25	25	24.8	24.92
20	25.2	24.6	24.4	24.6	24.4	24.64
30	23.1	23.9	23.9	24.2	24.1	23.84
40	23.8	23.6	23.7	23.8	24.2	23.8
	23.8	23.7	23.8	23.5	24.1	
50	23.6	23.5	24.1	23.4	23.3	23.5
	23.4	23.5	23.2	23.6	23.4	
60	22.9	23	22.8	22.7	22.8	22.97
	23.3	23.1	22.9	23.1	23.1	

Table 4-7:   Temperatures of the air at the exit of the channel with heater mounted on normal grey wall

Gap Size (mm)	Temperatures at the exit of the Channel (°C)					Average Temperature (°C)
10	27.8	27.2	26.9	27.5	26.1	27.1
20	25.8	27	27.1	26.8	25.5	26.44
30	25.8	26.2	26.7	27	27.8	26.7
40	24.6	26.6	27.2	27.4	29.2	26.99
	24.4	26.5	27.4	28.2	28.4	
50	29.6	30	31.1	31.9	31.1	29.5
	27.6	28.1	28.3	28.5	28.8	
60	28.2	28.5	28.6	28.5	28.3	28.1
	27.7	27.8	27.9	27.8	27.7	

data from tables 4-5, 4-6 & 4-7 above were also analysed for the determination of heat transfer components from the heater mounted at various gaps from the wall. Results of the analysis are presented in Table 4-8.

Table 4-8:   HT analysis with the heater mounted against the normal grey wall at various gaps

Gap Size $x\ 10^{-3}$ m	v m/s	T_{inlet} °C	T_{outlet} °C	T_{wall} °C	T_{inner} °C	T_{outer} °C	Pr	Gr	Ra=Gr*Pr	Nu_L	h W/(m².K)	Q_{cal} W	$Q_{rad-chan}$ W	Q_{out} W	$Q_{rad-out}$ W	Q_{tot} W	Q_{conv} W
10	0.2	24.9	27.1	54.0	102.1	95.9	0.7	1.2E+09	8.6E+08	88.8	4.2	2.4	100.6	105.6	158.6	367.2	108.0
20	0.3	24.6	26.4	51.5	100.7	95.3	0.7	1.2E+09	8.6E+08	88.8	4.2	7.2	101.2	104.5	157.3	370.2	111.7
30	0.3	23.8	26.7	47.7	98.2	94.2	0.7	1.2E+09	8.5E+08	88.7	4.2	17.8	101.1	102.6	155.2	376.6	120.3
40	0.2	23.8	27.0	47.4	97.8	94.0	0.7	1.2E+09	8.5E+08	88.7	4.2	21.9	100.7	102.2	154.6	379.5	124.1
50	0.2	23.5	29.5	47.4	96.5	93.4	0.7	1.2E+09	8.5E+08	88.6	4.2	33.9	97.4	101.2	153.4	385.8	135.1
60	0.2	23.0	28.1	47.0	96.4	92.9	0.7	1.2E+09	8.5E+08	88.6	4.2	32.6	98.0	100.4	152.8	383.8	132.9

Graphs illustrating the above outcome are displayed in Figure 4-1 which shows that the increase in channel gap size between the heater and the normal grey wall behind it resulted in

an increase of the overall performance of the heater approaching a maximum value around the gap of 50mm. The heater's efficiency at this point is about 35%. This means that the heater has sacrificed almost 15% of its overall performance with respect to the benchmark performance. This performance stays unchanged with further increase of the gap despite minor fluctuations that it may undergo.

All the other components of heat transfer from the heater's surfaces, namely the convection from the outer surface as well as the total net radiation heat loss from the outer and inner surfaces remained practically unchanged.
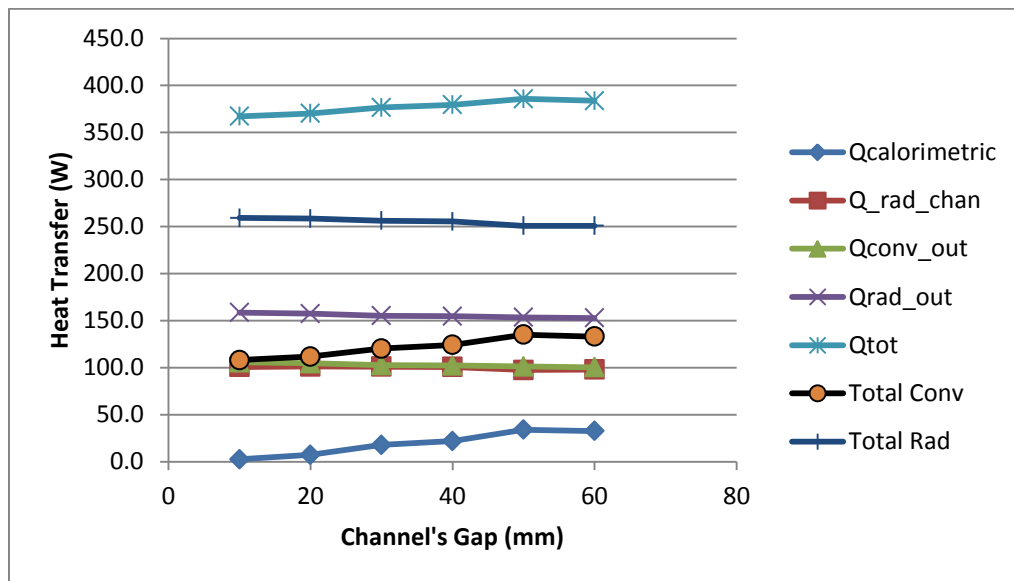
Figure 4-1: Heat transfer from the heater at various gaps with normal grey wall

Heater positioned in accordance to the manufacturer's recommendations.

The positioning of the heater with respect to the manufacturer's recommendations was captured during the execution of Experiment no.2. The heater's mounting met the height range of 200-300 mm from the floor and was 20 mm off-set from the wall. The performance of the heater is revealed in Table 4.13 produced by using the data displayed in Tables 4-9, 4-10,4-11 and Table 4-12, that were extracted from Tables 4-3, 4-5, 4-6 and 4-7 respectively.

Table 4-9: Heater's surfaces and wall temperatures for the 20mm gap: (a) in mV, (b) in °C

Gap Size(mm)	Normal Wall Temperatures (mV)			Gap Size(mm)	Normal Wall Temperature in °C		
	Wall	Inner	Outer		Wall	Inner	Outer
20	1.37	2.79	2.77	20	57.4	91.6	91.2
	1.11	3.24	2.94		51.1	102.5	95.3
	0.92	3.24	3.03		46.5	102.5	97.4
	1.10	3.39	3.03		50.9	106.1	97.4
				Average	51.5	100.7	95.3

38

Table 4-10:   Velocity of the air flow in m/s from the 20mm gap channel

Gap size (mm)	Velocity at the entry the channel (m/s)				Average Velocity
20	0.27	0.28	0.3	0.29	0.28	0.28

Table 4-11:   Temperature of the air in degrees Celsius at the channel's entry for a gap of 20mm

Gap Size (mm)	Temperatures at the entry of the Channel (^oC)					Av Temp (^oC)
20	25.2-	24.6	24.4	24.6	24.4	24.64

Table 4-12   Temperature of the air in degrees Celsius at the channel's exit for a gap of 20mm

Gap Size (mm)	Temperatures at the exit of the Channel (^oC)					Av Temp (^oC)
20	25.8	27	27.1	26.8	25.5	26.44

The following Table 4-13 is also an extract of Table 4-8 above.

Table 4-13:   Results of the analysis of the heater's performance for the 20mm Channel's gap

Gap Size $\times 10^{-3}$ m	v m/s	T_{inlet} ^oC	T_{outlet} ^oC	T_{wall} ^oC	T_{inner} ^oC	T_{outer} ^oC	Pr	Gr	Ra=Gr*Pr	Nu_L	h W/(m².K)	Q_{cal} W	$Q_{rad-chan}$ W	Q_{out} W	$Q_{rad-out}$ W	Q_{tot} W	Q_{conv} W
20	0.3	24.6	26.4	51.5	100.7	95.3	0.7	1.2E+09	8.6E+08	88.8	4.2	7.2	101.2	104.5	157.3	370.2	111.7

From Table 4-13 above, it can be seen that when the heater was mounted against the wall in accordance to the recommended position (20mm gap) by the manufacturer, its efficiency was

$$\eta_{conv} = \frac{Q_{conv}}{Q_{in}} \times 100 = \frac{111.7}{391} \times 100 = 28.6\%$$

In the position recommended by the manufacturer, the efficiency of the heater was lessened by approximately 30% compared to the benchmark efficiency figure of 41%. It can be seen in table 4.7 that the calorimetric heat transfer through the channel was 7.2W instead of 79.2W when compared to the freely mounted heater's performance (see table 4.1). Mounting the heater against the wall at the manufacturer's recommended position almost totally sacrificed the 'convective' heat transfer from the inner surface of the heater (approximately 91%) compared to the benchmark figures. In return, in this position more convective heat transfer was generated from the outer surface of the heater (104.5W), meaning a recovery of 32%, however it also meant higher heat transfer loss by radiation from the outer surface (157.3W compared to the benchmark figure of 113.7 W). In summary, mounting the heater on a wall reduces its efficiency.

Temperature profile of the air across the channel

An investigation of the air's temperature profile in the channel was conducted based on the temperature difference between the heater and the wall surface. The results displayed a temperature profile across the channel that supported the findings of La Pica et al. (1991) [25], although their geometry was different from the geometry in this research. The measured profiles display a temperature decrease from the heater's surface to a minimum value

somewhere near or approaching the middle of the gap, followed by an increase of the air temperature towards the wall. The results of experiment no. 2 indicated that at a gap of 50 mm the performance of the heater peaked, therefore the first measurement of the temperature profile of the air was effected at this position and Figure 4-2 displays the air's temperature profile measured across the boundaries of the channel.

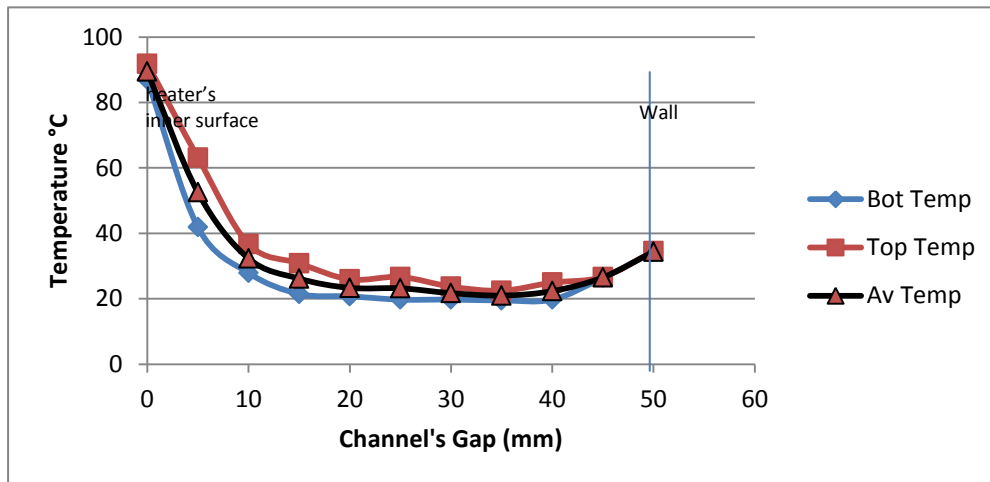Figure 4-2:   Temperature profile of the air across the channel at the 50mm gap between the heater and wall

Measurements of the air's temperature profile within the channel were taken for various gaps in the range of 10 to 50 mm. Figure 4-3 displays the results of these measurements.
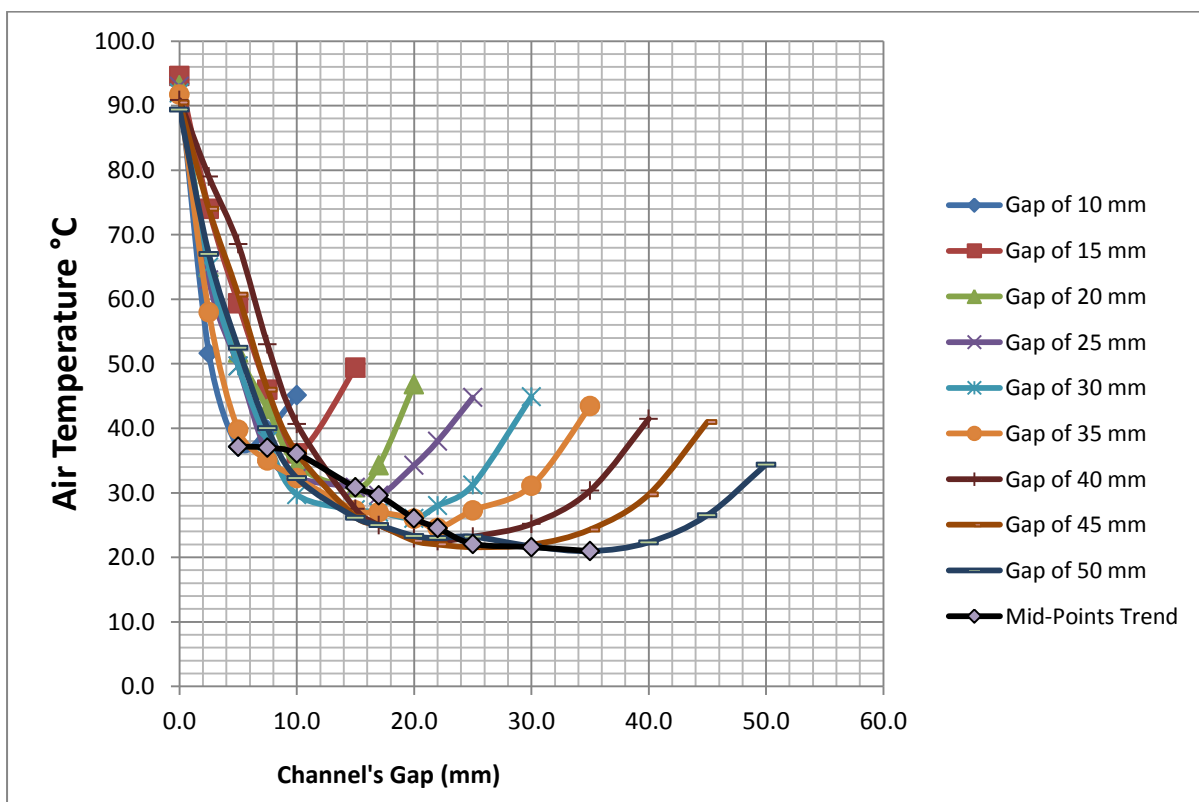

Figure 4-3: Temperature profiles as a function of increasing the size of the channel's gap at room temp of 20 °C.

It can be seen from Figure 4-3 that the minimum value of the air's temperature profile approaches the room's air temperature (20 °C), as the gap size increases.

The channel's gap of 50 mm therefore was determined as the optimum position for the mounting of the heater, when further experiments were to be performed regarding its performance. In other words the heater's performance for all future wall mounted tests will be obtained at this optimum position and compared to the benchmark value.

4.3.2   Experiment No. 3: Heater mounted at various heights from the floor

Table 4-14:   Temperatures of the heater's surfaces and of the wall at various heights from the floor

Height from floor (mm)	Normal Wall Temperatures (mV)			Height from floor (mm)	Normal Wall Temperature in °C		
	Wall	Inner	Outer		**Wall**	Inner	Outer
0	1.05	3.11	3.06	0	49.7	99.4	98.1
	1.07	3.11	2.95		50.2	99.3	95.5
	1.12	3.08	2.91		51.4	98.6	94.6
	1.07	3.13	2.73		50.2	99.8	90.2
	1.05	3.11	2.91		49.7	99.3	94.6
				Average	50.2	99.3	94.6
50	1.07	3.14	3.09	50	50.2	100.1	98.8
	1.18	3.05	2.93		52.8	97.8	94.9
	1.18	2.95	2.93		52.8	95.5	94.9
	1.16	3.04	2.93		52.3	97.8	94.9
	1.20	3.04	2.77		53.3	97.7	91.1
				Average	52.3	97.8	94.9
100	1.18	3.10	3.08	100	52.8	99.1	98.6
	1.18	3.07	2.94		52.8	98.4	95.3
	1.16	3.07	2.94		52.3	98.4	95.3
	1.13	3.07	2.94		51.6	98.4	95.3
	1.00	3.04	2.81		48.5	97.7	92.1
				Average	51.6	98.4	95.3
150	1.20	3.11	3.07	150	53.3	99.4	98.4
	1.16	3.10	2.93		52.3	99.0	94.9
	1.12	3.10	2.93		51.4	99.0	94.9
	0.96	3.10	2.91		47.5	99.0	94.5
	0.89	3.08	2.80		45.8	98.6	91.8
				Average	50.1	99.0	94.9
200	0.86	3.10	3.02	200	45.1	99.1	97.3
	0.94	3.10	2.88		47.1	99.1	93.9
	1.11	3.10	2.88		51.2	99.1	93.9
	1.17	3.10	2.88		52.6	99.1	93.9
	1.22	3.10	2.74		53.9	99.1	90.5
				Average	50.0	99.1	93.9
250	0.95	3.14	2.98	250	47.3	100.1	96.3
	1.08	3.07	2.90		50.4	98.5	94.7
	1.14	3.07	2.89		51.9	98.5	94.2
	1.08	3.07	2.88		50.4	98.5	93.7
	1.10	3.01	2.70		50.9	96.9	89.4
				Average	50.2	98.5	93.7
300	0.85	3.07	3.02	300	44.7	98.3	97.2
	1.06	3.03	2.97		49.8	97.4	96.0
	1.07	3.03	2.90		51.0	97.4	94.2
	1.03	3.03	2.90		49.1	97.4	94.2
	1.03	2.99	2.70		49.1	96.4	89.5
				Average	48.7	97.4	94.2

The heater was mounted at a distance of 50 mm away from the wall and further tests of its

Table 4-15:   Velocity of the air in m/s at the channel's inlet at various heights from the floor

Height from the floor	Air Velocity at Channel's Entry (m/s)					Average Velocity (m/s)
0 mm	0	0	0	0	0	0
50mm	0.09	0.1	0.1	0.11	0.11	0.102
	0.09	0.09	0.11	0.11	0.11	
100 mm	0.1	0.1	0.11	0.1	0.1	0.105
	0.1	0.11	0.11	0.12	0.1	
150 mm	0.13	0.14	0.15	0.14	0.13	0.14
	0.13	0.14	0.15	0.15	0.14	
200 mm	0.11	0.12	0.17	0.17	0.16	0.15
	0.12	0.11	0.17	0.19	0.18	
250 mm	0.15	0.16	0.17	0.17	0.15	0.158
	0.15	0.15	0.17	0.16	0.15	
300 mm	0.16	0.16	0.16	0.17	0.16	0.16
	0.16	0.15	0.16	0.17	0.15	

Tables 4-16 & 4-17 depict also the temperatures of the stream of air recorded at the entry and at the exit of the channel

Table 4-16:   Temperature of the air in °C at the channel's inlet and at various heights from floor

Height from floor (mm)	Air Temperature at Channel's Entry (°C)					Average Temperature (°C)
0	24	24	24	24	24	24
50	24	24	23.7	24.1	24	23.99
	24	24	24.1	24	24	
100	24.1	24.3	24.8	24.2	24.1	24.13
	23.9	24	24.1	23.9	23.9	
150	24.5	24.8	25.1	24.6	24.4	24.45
	24.6	24.3	24.2	24.1	23.9	
200	24.2	23.9	23.9	24	24	23.88
	23.8	23.9	23.8	23.7	23.6	
250	24.2	24	23.6	23.9	23.8	23.87
	24	23.8	23.8	23.8	23.8	
300	24.9	25	25	25.1	25.3	24.92
	24.9	24.8	24.5	24.8	24.9	

Table 4-17:   Temperature in °C of the air at the channel's outlet at various heights from the floor

Height from floor (mm)	Air Temperature at Channel's Exit (°C)					Av Temp (°C)
0	31.3	31.9	32.8	31.8	32.3	29.89
	29.1	27.2	27.5	26	29	
50	32	32	33.3	32.3	33.6	30.11
	25.7	27.3	28.2	27.6	29.1	
100	34.3	34.6	33	34.4	33	30.61
	26.4	27.9	28.7	26.7	27.1	
150	34.1	32.8	32	32.8	32.9	30.13
	26.6	27.4	27.9	28.2	26.6	
200	33.1	33.4	31	32.9	33.4	30.02
	27.4	27.6	28.1	26.7	26.6	
250	30.9	31	31.2	31.5	31.1	30.19
	26.8	31.2	28.9	31.5	27.8	
300	31.5	34.2	31.4	33.4	33.6	30.8
	27.2	30.4	28.7	29	28.6	

The analysis of the heater's performance was done from data of Tables 4-15, 4-16 and 4-17 and its outcome is presented in Table 4-18

Table 4-18:   Results of the analysis of the heater's performance at various heights from floor.

Height x 10^{-3} m	v m/s	Tinlet °C	Toutlet °C	Twall °C	Tinner °C	Touter °C	Pr	Gr	Ra=Gr*Pr	NuL	h W/(m^2.K)	Q_{Cal} W	Qrad chan W	Qout W	Qrad_out W	Qtot W	Q_{Conv} W
0	0.00	24.0	29.9	50.2	99.3	94.6	0.72	1.2E+09	8.5E+08	88.7	4.2	0.0	99.8	103.3	156.1	361.2	103.3
50	0.10	24.0	30.1	52.3	97.8	94.9	0.72	1.2E+09	8.6E+08	88.8	4.2	21.9	92.6	103.8	157.1	375.4	125.8
100	0.11	24.1	30.6	51.6	98.4	95.3	0.72	1.2E+09	8.6E+08	88.9	4.2	23.9	95.3	104.5	158.2	382.0	128.4
150	0.14	24.5	30.1	50.1	99.0	94.9	0.72	1.2E+09	8.6E+08	88.8	4.2	27.9	99.3	103.8	157.0	388.0	131.7
200	0.15	23.9	30.0	50.0	99.1	93.9	0.72	1.2E+09	8.5E+08	88.6	4.2	32.4	99.8	102.0	154.0	388.2	134.4
250	0.16	23.9	30.2	50.2	98.5	93.7	0.72	1.2E+09	8.5E+08	88.6	4.2	35.1	97.9	101.6	153.4	388.1	136.8
300	0.16	24.9	30.8	48.7	97.4	94.2	0.72	1.2E+09	8.6E+08	88.9	4.2	33.1	97.5	102.7	155.0	388.2	135.7

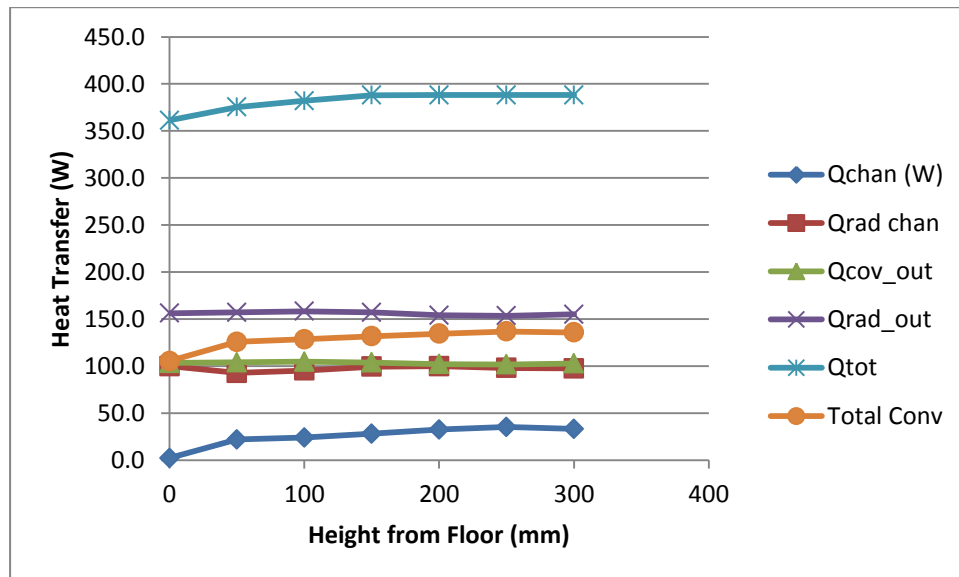Graphs drawn from the results of Table 4-18 are depicted in Figure 4.4.

Figure 4-4:   HT from the heater mounted at various heights from floor

Figure 4.4 reveals that the calorimetric heat through the channel is as expected zero when the heater is placed on the floor. From this zero starting point, the graph increases gradually towards its peak values around the heights of 200-300 mm. The second interesting observation is that the variation of the heater's mounting height, only affects the calorimetric heat transfer through the channel.

With regard to the outer surface of the heater, the effect of the vertical geometry changes was almost totally absent the overall heat transfer increased because of the convection heat increase directly attributed to the heat from the channel. The optimum height from the floor appears to be ~ 250mm.

4.3.3   **Experiment No. 4 The effect of changes of the surface conditions of the wall behind the heater.**

This experiment involved the change of emissivity of the wall behind the heater which would likely impact on the net radiation losses from the heater's inner surface and possibly affect the heat transfer to the air in the channel and the convection heat transfer from the heater's outer surface.

Black wall behind the heater

The heater was mounted at the optimum distance of 50 mm away from the wall which was painted with mat black paint and further tests of its performance under these conditions were carried out. The velocity of the air at the channel's inlet is shown in Table 4-19.

Table 4-19:   Velocity of the air in m/s at the channel's inlet with the heater mounted on a mat black wall

Gap Size (mm)	Air Velocity at Channel Entry (m/s)					Average Velocity (m/s)
50	0.22	0.27	0.27	0.26	0.22	0.238
	0.25	0.23	0.25	0.21	0.2	

Surface temperatures of the heater and the supporting wall are depicted in Table 4-20, both in millivolt records and their corresponding values in degrees Celsius.

Table 4-20:   Heater's and wall's surface temperatures at the channel's inlet with heater mounted on a mat black wall: (a) in mV, (b) in °C

Gap (mm)	Normal Wall Temperatures in(mV)			Gap (mm)	Normal Wall Temperature in °C		
	Wall	Inner	Outer		Wall	Inner	Outer
50	0.72	3.15	2.93	50	41.7	100.3	95.0
	1.12	3.03	2.89		51.4	97.5	94
	0.78	2.95	2.84		43.1	95.4	92.8
	1.01	2.91	2.78		48.7	94.6	91.4
	1.26	2.85	2.64		54.8	93.0	88.0
				Average	53.0	96.2	93.9

Temperatures of the air at the channel's inlet and outlet are displayed in Tables 4-20 and 4-21 respectively.

Table 4-21:   Temperature of the air in °C at the channel's inlet with the heater mounted on a mat black wall

Gap Size(mm)	Air Temperature at the Channel's Entry (°C)					Av Temperature (°C)
50	25.6	24.8	25.3	24.7	24.4	24.57
	25	24	23.9	24	24	

Table 4-22:   Temperature of the air in °C at the channel's outlet with the heater mounted on a mat black wall

Gap Size (mm)	Air Temperature at the Channel's Exit (°C)					Av Temp (°C)
50	32.3	32.3	31	31.4	26.4	28.98
	26.8	28	28.3	26.5	26.8	

The summary of the analysis of the data is presented in Table 4-23.

Table 4-23:   Results of the analysis of the heater's performance when mounted against the mat black wall

Gap Size	v	T_{inlet}	T_{outlet}	T_{wall}	T_{inner}	T_{outer}	Pr	Gr	Ra=Gr*Pr	Nu_L	h	Q_{cal}	$Q_{rad-chan}$	Q_{out}	$Q_{rad-out}$	Q_{tot}	Q_{conv}
x 10^{-3}m	m/s	°C	°C	°C	°C	°C					$W/(m^2.K)$	W	W	W	W	W	W
50	0.24	25	29	53	96	92	0.721	1.1E+09	8.2E+08	87.8	4.2	36.8	107.9	96.8	146.9	388.5	133.7

The painted mat black wall behind the heater absorbs the total radiation emitted from the inner surface facing it. Part of this absorption helped warm up the air of the channel which affected the calorimetric heat transfer through the channel. The amount of calorimetric HT through the channel, when compared to the condition of normal grey wall behind the heater, has undergone a small improvement (nearly 9%), although an overall decrease of more than 52% with respect to the maximum performance (freely-mounted) or benchmark condition. However the main effect of the overheating of the wall due to the total absorption of the radiation is the tendency of the heat to get dissipated through the wall by conduction HT.

The heater's overall performance when mounted on the mat black wall, is similar to that displayed when was mounted on the normal grey wall.

Black Insulated Wall behind the Heater

The heater was mounted at a distance of 50 mm away from the insulated black wall behind it and further tests of its performance were conducted. Data were recorded in the same way as previous arrangements.

The heater's and wall's surface temperatures are presented in Table 4-27

Table 4-24:   Surfaces temperature with the heater mounted on a black insulated wall: (a) in mV, (b) in °C

Gap Size(mm)	Normal Wall Temperatures in mV			Gap Size(mm)	Normal Wall Temperature in °C		
	Wall	Inner	Outer		Wall	Inner	Outer
50	1.8	3.32	2.89	50	67.8	104.3	94.0
	1.64	3.31	2.83		64.0	104.3	92.1
	1.58	3.3	2.81		62.5	103.9	92.5
	1.52	3.19	2.73		61.1	101.4	90.2
	1.5	2.9	2.6		60.5	94.2	87.0
				Average	63.2	101.6	91.1

The velocity of the air at the channel's entry and exit are displayed in Tables 4-24, 4-25 and 4-26 respectively.

Table 4-25:   Velocity of the air in m/s at the channel's inlet with the heater mounted on a black insulated wall

Gap Size (mm)	Air velocity at the channel's entry (m/s)					Av velocity (m/s)
50	0.21	0.22	0.23	0.22	0.21	0.21
	0.19	0.2	0.21	0.21	0.2	

Table 4-26:   Temperature of the air in °C at the channel's inlet with the heater mounted on a black insulated wall

Gap Size(mm)	Air temperature at the channel's entry (°C)					Av temperature (°C)
50	24.4	25.6	25	24.5	24.2	24.44
	24	24.4	24.3	24.1	23.9	

Table 4-27:   Temperature of the air in °C at the channel's outlet with the heater mounted on a black insulated wall

Gap Size (mm)	Airflow Temperature at Channel Exit (°C)					Av Temp (°C)
50	31.8	30	28	29.5	30.5	29.6
	26.4	40	31.5	32.2	25.7	

The summary of the analysis of the data is presented in Table 4-28.

Table 4-28:   Components of HT from the heater's when mounted against the black insulated wall

Gap Size x 10^{-3} m	v m/s	T_{inlet} °C	T_{outlet} °C	T_{wall} °C	T_{inner} °C	T_{outer} °C	Pr	Gr	Ra=Gr*Pr	Nu_L	h W/(m^2.K)	Q_{cal} W	$Q_{rad-chan}$ W	Q_{out} W	$Q_{rad-out}$ W	Q_{tot} W	Q_{conv} W
50	0.21	24.4	29.6	63	102	91	0.72	1.2E+09	8.3E+08	88.2	4.2	38	102	97	146	383	135

Table 4.28 displays the various heat transfer components for the arrangement of the heater mounted on a high emissivity insulated wall. It can be noticed that the channel's calorimetric HT of almost 20% reflects an improvement of more than 12% comparatively to the normal grey wall condition, but just a symbolic improvement of less than 4% with respect to the black-non-insulated wall condition. Meanwhile the overall performance remained almost unchanged comparatively to the condition of black-non-insulated wall condition behind the heater.

Shiny Wall

Aluminium foil of emissivity 0.05 was used to make the wall behind the heater highly reflective. The heater was mounted with an off-set of 50 mm from the wall and further tests of its performance were conducted. In this condition the velocity of the air through the channel is depicted in Table 4-29.

Table 4-29:   Velocity of the air in m/s at the channel's inlet with the heater mounted on a highly reflective wall

Gap Size (mm)	Air Velocity at the Channel's Entry (m/s)					Av Velocity (m/s)
50	0.2	0.19	0.21	0.2	0.17	0.19
	0.18	0.18	0.2	0.19	0.18	

Temperature of the air through the channel measured at the channel's inlet and outlet is displayed in Tables 4-30 and 4-31 respectively.

Table 4-30:   Temperature of the air at the channel's inlet with the heater mounted on a highly reflective wall

Gap Size(mm)	Temperature of the air at the channel's entry (°C)					Av temperature (°C)
50	25	25.3	25.2	25.1	25.1	25.5
	24.7	25.1	25.1	25	24.9	

Table 4-31:   Temperature of the air at the channel's outlet with the heater mounted on a highly reflective wall

Gap Size (mm)	Temperature of the air at the Channel's exit (°C)					Av Temp (°C)
50	28.2	33.7	36.2	36.2	36.4	31.14
	25.6	27.7	28.7	30.4	28.3	

The Heater's Surface temperatures and those of the wall are depicted in Table 4-32.

Table 4-32:   Heater's and wall's temperature when mounted on a highly shiny wall: (a) in mV, (b) in °C

Gap Size(mm)	Normal Wall Temperatures (mV)			Gap Size(mm)	Normal Wall Temperature in °C		
	Wall	Inner	Outer		Wall	Inner	Outer
50	0.48	3.74	3.31	50	35.9	114.6	104.3
	0.44	3.68	3.3		34.9	113.1	104.0
	0.43	3.63	3.24		34.5	111.9	102.5
	0.39	3.57	3.12		33.5	110.6	99.7
	0.34	3.44	3.02		32.4	107.3	97.2
				Average	34.3	111.5	101.5

The analysis of the data above bore out the heat transfer results presented in Table 4-33

Table 4-33:   Results of the analysis of the heater's performance when mounted against the shiny wall

Gap Size $\times 10^{-3}$m	v m/s	T_{inlet} °C	T_{outlet} °C	T_{wall} °C	T_{inner} °C	T_{outer} °C	Pr	Gr	Ra=Gr*Pr	Nu_L	h W/(m².K)	Q_{cal} W	$Q_{rad-chan}$ W	Q_{out} W	$Q_{rad-out}$ W	Q_{tot} W	Q_{conv} W
50	0.19	25.1	31.1	34.3	111.5	101.5	0.72	1.3E+09	9.1E+08	90.1	4.3	40.6	6.5	115.8	177.1	339.9	156.3

According to the results in Table 4.33 covering the portion of the wall where the heater is mounted, with aluminium foil (emissivity = 0.05) enabled a global recovery of nearly all its efficiency that was sacrificed by mounting the heater on the wall (97%), when compared to the benchmark value. With an improvement of almost 20% of the calorimetric HT through the channel and nearly 15% increase of natural convection heat transfer at the heater's outer surface, meaning an overall improvement of 16% of the heater's efficiency compared to the normal grey wall condition, the heater performed better in this wall mounted condition. The 20% improvement inside the channel is probably explained by the fact that the nett radiation heat loss from the heater's hot-inner-surface facing the wall is reduced due to the shiny wall The heater's inner surface undergoes a temperature increase, which subsequently enhances the transfer of calorimetric heat to the air rising in the channel's space. The heater's inner surface temperature rise also affects the temperature of the outer surface of the heater which also experiences a temperature rise. This temperature increase at the outer surface

subsequently enhances the convection HT from the outer surface (15%), however it generates an increase of radiation heat transfer loss to the enclosure's walls.

In summary, by making the wall behind the heater shiny, the overall efficiency of the heater was shifted or increased to 40%, bringing it closer to the 41% which is the benchmark based on the freely standing condition within the enclosure.

The overall comparison of the heater's performance resulting from the various experiments is displayed in Figure 4-8
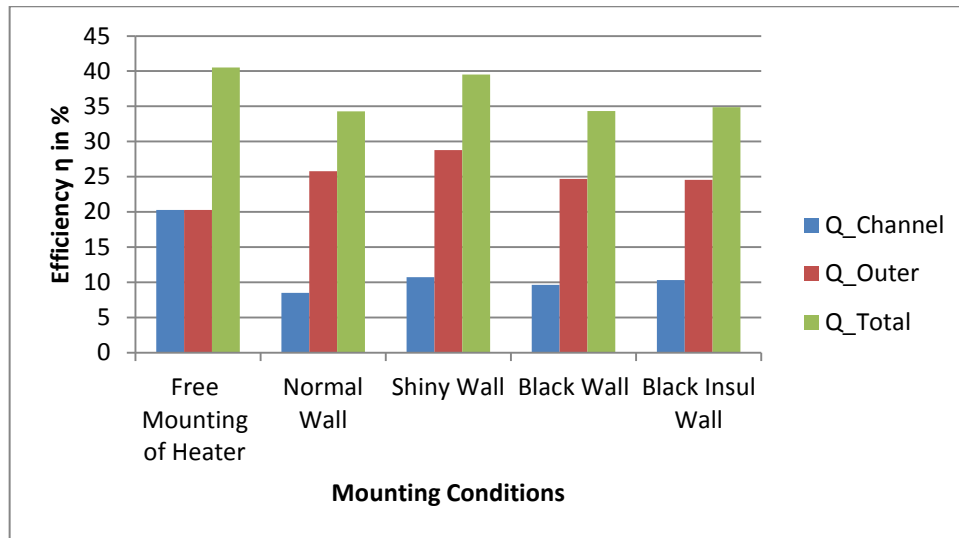
Figure 4-5:   Efficiencies of the Heater with respect to its mounting conditions

4.4   **Summary**

The various experiments performed in this Chapter, yielded data which were evaluated with the pertinent equations and empirical correlations presented in Chapter 2. Analyses of the data resulted in outcomes presented in tables and graphs, with commentary on the behaviour of the various modes of heat transfer from the space heater and its performance or efficiency associated or influenced by the various geometries of mounting it on the wall.

CHAPTER 5

CONCLUSIONS AND RECOMMENDATIONS

1.1   Conclusions

The research work presented in this dissertation aimed at investigating and possibly optimizing the performance of the wall mounted space comfort heater. The rationale was to perform tests at various mounting geometries (heights of the heater from the floor and its gaps from the wall). The influence of various conditions of the surface of the wall behind the heater (highly reflective, mat black and mat black- insulated) in the overall heater's performance was also investigated. To this end all objectives were accomplished.

Numerous studies of the heat transfer from a vertical plate and on parallel vertical walls have been reported in the literature, but none of them catered for this project's geometry as well as the conditions of the surface of the wall supporting the space heater.

The channel formed by the heater and the wall against which it was mounted has been the key or major issue of interest in this study. Profiles of the temperature of the air across the channel's gaps were instrumental in improving the understanding of the heat transfer phenomenon in this geometry. In order to address the research problems, the following three main models were used for the evaluation of the various components of HT from the heater:

- The equation proposed by Churchill and Chu applicable for a wide range of Rayleigh numbers was used for the calculation of the quantities of free convective heat transfer mode at the outer surface of the heater.
- The calorimetric approach or method was used in order to determine the heat imparted to the ambient air as it flowed through the channel created by the heater being mounted on the enclosure's wall
- The equation for the net radiation heat transfer between two infinitely parallel vertical surfaces and from a vertical surface that does not see any part of itself surrounded by an enclosure, were used for the evaluation of the net radiation heat transfer inside the channel and from the outer surface of the heater to the surrounding enclosure's walls respectively.

It was found that the heater's height above 200mm from the floor was enough for the full stream of cold air to get into the channel. It was found that the gap of 50mm was the

minimum distance from the wall allowing the heater to reach its best efficiency when mounted.

The heater transferred a maximum amount of heat from its two faces when it was placed vertically in the middle of the enclosure. Its efficiency in this position was 41%. When mounted against the wall, it was found that the heater sacrificed almost the total amount of heat transfer from its surface facing the wall, by keeping only 6% of it, even though a portion of this loss (16%) was recovered from its outer surface.

The black, black-insulated and shiny transformations on the surface of the wall behind the heater affected the heater's performance as described below:

With the black wall

Advantages:

- Affordable.
- Easy to achieve.

Disadvantage:

- No effective improvement in the overall HT to the enclosure.

Recommendation:

- This transformation is irrelevant

With the black insulated wall.

Advantages:

- None.

Disadvantages:

- Relatively expensive to achieve.
- No effective improvement in the overall HT to the exposure.

Recommendation:

- This transformation is irrelevant.

With the reflective wall:

Advantages:

- Affordable.
- Easy to achieve.

- Preserved the aesthetic of the heater's mounting.
- Improved the performance of the heater at both channel side and outer surface and hence the overall performance.

Disadvantage:
- Increased radiation loss at the outer surface of the heater

Recommendation:

This transformation is highly relevant because it ensured the aesthetic of the mounting, and increased the efficiency of the heater by almost equalling its benchmark value.

1.2 Final recommendation

The flow inside the channel that is created by an isothermal vertical surface mounted on a wall needs to be researched further with the aim to eventually build up a scientific model that would cater for the geometry.

REFERENCES

[1]   Japanese style, 2016, 'history of the kotatsu table', available online:
http://www.japanesestyle.com/archive/home/history-kotatsu-table [Date accessed: 8 July
2016].

[2]   Econo-Heat, 2016, Available Online: http://econo-heat.com/za/company-history/
[Date accessed: 8 July 2016].

[3]   eheat, 2016, 'World's best wall mounted panel heaters',
available online: http://www.eheat.com/ [Date accessed: 12 June 2016].

[4]   Eckert, E.R.G. and Carlson, W.O., 1960, "Natural convection in an air layer enclosed between
two vertical plates with different temperatures", International journal of heat and mass transfer,
2, Issues 1–2, pp 106–120, available online:
http://www.sciencedirect.com/science/article/pii/0017931062900820, [Date accessed: 1
November   2014].

[5]   Krishnan, A.S., Premachandran, B., Balaji, C. and Venkateshan, S.P., 2004, "Combined
Experimental and Numerical Approaches to Multi-mode Heat Transfer between Vertical
Parallel Plates". Experimental Thermal and Fluid Science, **29**, Issue 1, pp. 75–8. available
online:
http://www.sciencedirect.com/science/article/pii/S089417770400038X [Date accessed: 20 June
2014].

[6]   Linhui, C., Huaizhang, T., Yanzhong, L. and Dongbin, Z., 2006, "Experimental Study on
Natural Convective Heat Transfer from a Vertical Plate with Discrete Heat Sources Mounted
on the Back", Energy Conversion and Management, **47**, pp 3447–3455. Available Online:
https://www.researchgate.net/publication/245159853_Experimental_study_on_natural_convecti
ve_heat_transfer_from_a_vertical_plate_with_discrete_heat_sources_mounted_on_the_back
[Date accessed: 6 July 2016].

[7]   Sandberg, M. and Moshfegh, B., 2002, "Buoyancy-induced Air Flow in Photo-voltaic Facades,
Effect of Geometry of the Air Gap and Location of Solar Cell Modules", Building and
Environment, **37**, pp 211–218. available online:
https://www.researchgate.net/publication/245145314_Buoyancy-
induced_air_flow_in_photovoltaic_facades [Date accessed: 6 June 2016].

[8]   Moshfegh, B. and Sandberg, M., 1998, "Flow and heat transfer in the air gap behind photovoltaic panels", Renewable and Sustainable Energy Reviews, **2,** pp 287–301. available online: https://www.researchgate.net/publication/227421632_Flow_and_heat_transfer_in_the_air_gap_ behind_photovoltaic_panels [Date accessed: 6 June 2016].

[9]   Karlekar, B.V. and Desmond, R.M., 1982, *Heat Transfer*. West Publishing CO, Minnesota, USA.

[10]   CENGEL, A.Y. and Ghajar A.J., 2015, *Heat and Mass Transfer: Fundamentals and Applications*, McGraw-Hill Education, New York.

[11]   Simonson, J.R., 1983, *Engineering Heat Transfer*. Macmillan Press Ltd, London, UK.

[12]   Bejan, A., 1993, Heat Transfer. John Wiley and Sons, Inc., USA.

[13]   Gryzagoridis, J., 1971, "Natural Convection from a Vertical Flat Plate in the Low Grashof Number Range", International Journal of Hear and Mass Transfer, **14**, pp. 162-165. available online: http://www.worldpapercat.com/1747/Article4306972.htm [Date accessed: 4 December 2013].

[14]   Holman, J.P., 2010, *Heat Transfer*, McGraw-Hill Education, New York.

[15]   Ghoshdastidar, P.S., *Heat Transfer*, 2007, Oxford University Press, New Delhi, India

[16]   Incropera, F.P., Dewitt, D.P., Bergman, T.L. and Lavine A.S., 2006, *Fundamentals of Heat and Mass Transfer*. John Wiley & Sons Inc, New Jersey, USA.

[17]   Howell, J.R, Menguc, M.P, Siegel, R., 2016, *Thermal Radiation Heat Transfer*, CRC Press, Taylor and Francis Group, LLC, Boca Raton, USA. available online: https://books.google.co.za/books?id=aeSYCgAAQBAJ&printsec=frontcover&source=gbs_vpt _reviews#v=onepage&q&f=false [Date accessed: 14 July 2016].

[18]   Sable, M.J., Jagtap, S.J., Patil, P.S., Baviskar, P.R. and Barve, S.B., 2010, "Enhancement Of Natural Convection Heat Transfer On Vertical Heated Plate By Multiple V-Fin Array", International Journal of Research & Reviews in Applied Sciences, **5**, Issue 2, p123. available online: http://www.arpapress.com/volumes/vol5issue2/ijrras_5_2_04.pdf [Date accessed: 3 July 2014].

[19]   Comunelo, R. and Güths, S., 2005, "Natural Convection at Isothermal Vertical Plate: Neighborhood Influence", 18th International Congress of Mechanical Engineering, November

6-11, 2005, Ouro Preto, MG. available online: http://www.lmpt.ufsc.br/publicacao/86.pdf [Date accessed: 6 July 2015].

[20] Kreith, F., Manglik, R.M. and Bohn, M.S., 2011, *Principles of Heat Transfer*, Cengage Learning, Stanford USA.

[21] TSI, 2016, Velocicalc Air Velocity Meter 9535, available online: http://www.tsi.com/VELOCICALC-Air-Velocity-Meter-9535/ [Date accessed: 11 June 2015].

[22] Accuracy of the 9515Velocity Meter, available online: http://www.tsi.com/uploadedFiles/_Site_Root/Products/Literature/Spec_Sheets/9515-9535-9545-VelociCalc_US_2980569-web.pdf [Date accessed: 16 February 2017].

[23] Fluke, n.d., Thermocouple Voltage to Temperature Calculator, available online: http://us.flukecal.com/Thermocouple-Temperature-Calculator [Date accessed: 20 November 2015].

[24] Zeal, 2015, General Catalogue, available online: https://www.zeal.co.uk/pdf/Zeal_General_Catalogue_2015.pdf. [Date accessed: 12 July 2016].

[25] La Pica, A., Rodono, G. and Volpes, R. 1993, "An Experimental Investigation on Natural Convection of Air in a Vertical Channel", International Journal of Heat and Mass Transfer, **36**, Issue 3, pp 611-616 available online: https://www.researchgate.net/file.PostFileLoader.html?id=530ede36d685ccdd2c8b4579&assetKey=AS%3A272440071000081%401441966182461 [Date accessed: 12 July 2016].

[26] Omega, n.d., Revised Thermocouple Reference Tables, available online: https://es.omega.com/temperature/pdf/Type_K_Thermocouple_Reference_Table.pdf [Date accessed: 15 February 2016].

APPENDIX A
Air properties at atmospheric pressure [10]

Properties of air at 1 atm pressure

Temp. T, °C	Density ρ, kg/m³	Specific Heat c_p, J/kg·K	Thermal Conductivity k, W/m·K	Thermal Diffusivity α, m²/s	Dynamic Viscosity μ, kg/m·s	Kinematic Viscosity ν, m²/s	Prandtl Number Pr
−150	2.866	983	0.01171	4.158×10^{-6}	8.636×10^{-6}	3.013×10^{-6}	0.7246
−100	2.038	966	0.01582	8.036×10^{-6}	1.189×10^{-5}	5.837×10^{-6}	0.7263
−50	1.582	999	0.01979	1.252×10^{-5}	1.474×10^{-5}	9.319×10^{-6}	0.7440
−40	1.514	1002	0.02057	1.356×10^{-5}	1.527×10^{-5}	1.008×10^{-5}	0.7436
−30	1.451	1004	0.02134	1.465×10^{-5}	1.579×10^{-5}	1.087×10^{-5}	0.7425
−20	1.394	1005	0.02211	1.578×10^{-5}	1.630×10^{-5}	1.169×10^{-5}	0.7408
−10	1.341	1006	0.02288	1.696×10^{-5}	1.680×10^{-5}	1.252×10^{-5}	0.7387
0	1.292	1006	0.02364	1.818×10^{-5}	1.729×10^{-5}	1.338×10^{-5}	0.7362
5	1.269	1006	0.02401	1.880×10^{-5}	1.754×10^{-5}	1.382×10^{-5}	0.7350
10	1.246	1006	0.02439	1.944×10^{-5}	1.778×10^{-5}	1.426×10^{-5}	0.7336
15	1.225	1007	0.02476	2.009×10^{-5}	1.802×10^{-5}	1.470×10^{-5}	0.7323
20	1.204	1007	0.02514	2.074×10^{-5}	1.825×10^{-5}	1.516×10^{-5}	0.7309
25	1.184	1007	0.02551	2.141×10^{-5}	1.849×10^{-5}	1.562×10^{-5}	0.7296
30	1.164	1007	0.02588	2.208×10^{-5}	1.872×10^{-5}	1.608×10^{-5}	0.7282
35	1.145	1007	0.02625	2.277×10^{-5}	1.895×10^{-5}	1.655×10^{-5}	0.7268
40	1.127	1007	0.02662	2.346×10^{-5}	1.918×10^{-5}	1.702×10^{-5}	0.7255
45	1.109	1007	0.02699	2.416×10^{-5}	1.941×10^{-5}	1.750×10^{-5}	0.7241
50	1.092	1007	0.02735	2.487×10^{-5}	1.963×10^{-5}	1.798×10^{-5}	0.7228
60	1.059	1007	0.02808	2.632×10^{-5}	2.008×10^{-5}	1.896×10^{-5}	0.7202
70	1.028	1007	0.02881	2.780×10^{-5}	2.052×10^{-5}	1.995×10^{-5}	0.7177
80	0.9994	1008	0.02953	2.931×10^{-5}	2.096×10^{-5}	2.097×10^{-5}	0.7154
90	0.9718	1008	0.03024	3.086×10^{-5}	2.139×10^{-5}	2.201×10^{-5}	0.7132
100	0.9458	1009	0.03095	3.243×10^{-5}	2.181×10^{-5}	2.306×10^{-5}	0.7111
120	0.8977	1011	0.03235	3.565×10^{-5}	2.264×10^{-5}	2.522×10^{-5}	0.7073
140	0.8542	1013	0.03374	3.898×10^{-5}	2.345×10^{-5}	2.745×10^{-5}	0.7041
160	0.8148	1016	0.03511	4.241×10^{-5}	2.420×10^{-5}	2.975×10^{-5}	0.7014
180	0.7788	1019	0.03646	4.593×10^{-5}	2.504×10^{-5}	3.212×10^{-5}	0.6992
200	0.7459	1023	0.03779	4.954×10^{-5}	2.577×10^{-5}	3.455×10^{-5}	0.6974
250	0.6746	1033	0.04104	5.890×10^{-5}	2.760×10^{-5}	4.091×10^{-5}	0.6946
300	0.6158	1044	0.04418	6.871×10^{-5}	2.934×10^{-5}	4.765×10^{-5}	0.6935
350	0.5664	1056	0.04721	7.892×10^{-5}	3.101×10^{-5}	5.475×10^{-5}	0.6937
400	0.5243	1069	0.05015	8.951×10^{-5}	3.261×10^{-5}	6.219×10^{-5}	0.6948
450	0.4880	1081	0.05298	1.004×10^{-4}	3.415×10^{-5}	6.997×10^{-5}	0.6965
500	0.4565	1093	0.05572	1.117×10^{-4}	3.563×10^{-5}	7.806×10^{-5}	0.6986
600	0.4042	1115	0.06093	1.352×10^{-4}	3.846×10^{-5}	9.515×10^{-5}	0.7037
700	0.3627	1135	0.06581	1.598×10^{-4}	4.111×10^{-5}	1.133×10^{-4}	0.7092
800	0.3289	1153	0.07037	1.855×10^{-4}	4.362×10^{-5}	1.326×10^{-4}	0.7149
900	0.3008	1169	0.07465	2.122×10^{-4}	4.600×10^{-5}	1.529×10^{-4}	0.7206
1000	0.2772	1184	0.07868	2.398×10^{-4}	4.826×10^{-5}	1.741×10^{-4}	0.7260
1500	0.1990	1234	0.09599	3.908×10^{-4}	5.817×10^{-5}	2.922×10^{-4}	0.7478
2000	0.1553	1264	0.11113	5.664×10^{-4}	6.630×10^{-5}	4.270×10^{-4}	0.7539

Linear interpolation- of air properties at the intermediate temperatures of 52.3°C [20]

INTERPOLATION OF AIR PROPERTIES AT FILM TEMPERATURE						
Temperature (t)	Density (ρ)	Specific Heat (C_p)	Thermal Conductivity (k)	Kinematic viscosity (v)	Expansion Coefficient (β)	Prandtl Number (Pr)
°C	kg/m³	kJ/kg.K	W/(m.K)	x 10^{-6} m²/s	x 10^{-3} (1/K)	
50	1.092	1.007	0.02735	17.98	3.1	0.7228
51.6763	1.086468	1.007	0.027472	18.14428	3.083237	0.722364
60	1.059	1.007	0.02808	18.96	3	0.7202

Revised Thermocouple Reference Tables

J

Nickel-Chromium
vs.
Nickel-Aluminum

TYPE K

Reference Tables
N.I.S.T.
Monograph 175
Revised to
ITS-90

MAXIMUM TEMPERATURE RANGE
Thermocouple Grade
– 200 to 1250°C, – 328 to 2282°F
Extension Grade
0 to 200°C, 32 to 392°F
LIMITS OF ERROR
(whichever is greater)
Standard: 2.2°C or 0.75% Above 0°C
2.2°C or 2.0% Below 0°C
Special: 1.1°C or 0.4%
COMMENTS, BARE WIRE ENVIRONMENT:
Clean Oxidising and Inert, Limited Use in
Vacuum or Reducing, Wide Temperature
Range, Most Popular Calibration
TEMPERATURE IN DEGREES °C
REFERENCE JUNCTION AT 0°C

Thermoelectric Voltage in Millivolts

56

APPENDIX C

Calculations on the heater's performance at gap size of 50 mm

1) <u>Records in mV</u>.

Table C-1: Temperature recorded in mV with heater mounted on normal wall

Gap Size (mm)	Normal wall Temperatures (mV)		
	Wall	Inner	Outer
50	1.15	3.06	2.95
	0.97	3.06	2.86
	0.82	3.09	2.76
	0.9	2.76	2.89

2) <u>Conversion from mV into °C</u>

From the conversion table:

The millivolt equivalent of the room temperature is: 0.96mV.

The absolute value of the above temperature in mV is: 1.15 + 0.96 = 2.11mV

Read from the table of Appendix B, 2.11mV falls between 2.106 and 2.147mV corresponding to temperatures in °C of 52 and 53°C respectively.

Applying the linear interpolation gives:

$$t_{2.11} = \frac{2.11 - 2.106}{2.147 - 2.106}(53 - 52) + 52 = 52.1°C$$

The conversion is straight forward with the online converter;

The mV value of 1.15mV is inputted to the converter (Thermocouple (mV)) with assurance taken that the room temperature (Reference Junction Temperature) was set at 24°C and that the thermocouple was selected correctly as the Type K, the result pops out exactly 52.1°C.

The conversion through the same process of all the values in the respective columns of the Wall, Inner and Outer surfaces respectively of the table above, gives the following table of converted values:

Table C-2:   Temperature converted in °C with heater mounted on normal wall

Gap Size (mm)	Temperatures of respective surfaces in °C		
	Wall	Inner	Outer
50	52.1	98.1	95.4
	47.6	98.1	93.4
	44.0	98.8	90.8
	45.9	90.8	94.0

Hence the average temperature of each surface for the 50mm gap is:

Table C-3: Average temperature in °C with heater mounted on normal wall

Gap Size (mm)	Temperatures of respective surfaces in °C		
	Wall	Inner	Outer
Average temperature for 50mm gap	47.4	96.5	93.4

3) Other measurements through the channel

At this gap of 50mm and for the airflow through the channel, the tables of its: i) velocity of at entry of channel, ii) temperature at entry of channel, and iii) temperature at exit of channel are respectively the following, with their respective averages given on their last columns:

Table C-4: Velocity at entry of channel in m/s with heater mounted on normal wall

Gap size (mm)	Velocity at the entry the channel (m/s)					Average velocity
50	0.15	0.15	0.16	0.16	0.14	0.16
	0.15	0.2	0.18	0.16	0.15	

Table C-5: Temperature at channel inlet in °C with heater mounted on normal wall

Gap Size (mm)	Temperatures at the entry of the Channel (oC)					Average Temperature (oC)
50	23.6	23.5	24.1	23.4	23.3	23.5
	23.4	23.5	23.2	23.6	23.4	

Table C-6: Temperature at channel outlet in °C with heater mounted on normal wall

Gap Size (mm)	Temperatures at the exit of the Channel (oC)					Average Temperature (oC)
50	29.6	30	31.1	31.9	31.1	29.5
	27.6	28.1	28.3	28.5	28.8	

4) Calorimetric heat transferred through the channel

Equations (2-12) and (2-11) apply:

$$\dot{m} = \rho_{inlet} v_{inlet} A_c \ \text{ and } \ \dot{Q}_{cal} = \dot{m} C_{p_{inlet}} (T_{outlet} - T_{inlet}).$$

$\dot{m}$ was chosen to be evaluated at the inlet of the channel because of the continuity of the mass flow rate of air through the channel.

Due to the relatively small temperature difference between the inlet and the outlet of the channel in this case (around 6°C), the specific heat of the airflow was likely to stay constant through the channel. Hence the air properties involved (density and specific heat) were selected at inlet temperature.

i)   Air properties at channel inlet

The inlet average temperature of 23.5°C falls between 20 and 25°C (see Appendix A). The interpolator of air properties at 23.5°C displays the following:

Table C-7: Determination of air properties at 23.5°C through the linear interpolator

INTERPOLATION OF AIR PROPERTIES OF THE INLET TEMPERATURE						
T	ρ	Cp	k	v	β	Pr
°C	kg/m3	kJ/kg.K	W/(m.K)	$\times 10^{-6}$ m²/s	$\times 10^{-3}$ (1/K)	
20	1.204	1.007	0.02514	15.16	3.43	0.7309
23.5	1.19	1.007	0.025399	15.482	3.38975	0.72999
25	1.184	1.007	0.02551	15.62	3.3725	0.7296

So $\rho_{inlet} = 1.19$ kg/m3 and $C_P = 1007$ J/kg/K

    ii)   <u>Mass flow rate of air through the channel ($\dot{m}$):</u>

The cross-sectional of the channel: $A_C = 50 \times 10^{-3} \times 0.588 = 0.0294 m^2$

The mass flor rate of air through the channel is then:

$$\dot{m} = \rho_{inlet} \times v_{inlet} \times A_C = 1.19 \times 0.16 \times 0.0294 = 0.056 kg/s$$

    iii)   The calorimetric heat transfer is given by:

$$\dot{Q}_{Cal} = \dot{m} \times C_P (T_{Outlet} - T_{Inlet}) = 0.056 \times 1007 \times (29.5 - 23.5) = 33.82 W$$

    5) Convection at the Outer surface.

    i)   The film temperature at the outer surface is:

$$T_{Film} = \frac{T_{Out} + T_{Room}}{2} = \frac{93.4 + 24}{2} = 58.7°C$$

    ii)   Properties of air at 58.7°C:

    iii)   Linear interpolation of air at properties film temperature

Table C-8: Determination of air properties at 58.7°C through the linear interpolator

INTERPOLATION OF AIR PROPERTIES AT FILM TEMPERATURE						
T	ρ	Cp	k	v	β	Pr
°C	kg/m3	kJ/kg.K	W/(m.K)	$\times 10^{-6}$ m²/s	$\times 10^{-3}$ (1/K)	
50	1.092	1.007	0.02735	17.98	3.1	0.7228
58.7	1.06329	1.007	0.027985	18.8326	3.013	0.720538
60	1.059	1.007	0.02808	18.96	3	0.7202

    iv)   <u>Grashof number:</u>

$$Gr_L = \frac{9.81 \times 3.013 \times 10^{-3} \times (93.4 - 24) \times 0.588^3}{(18.8326 \times 10^{-6})^2} = 1.176 \times 10^9$$

v) <u>Rayleigh number</u>

$$Ra_L = 1.176 \times 10^9 \times 0.720538 = 0.85 \times 10^9$$

vi) <u>Nusselt number</u> (Correlation of Churchill and Chu applies)

$$Nu_L = 0.68 + \frac{0.67 \times (0.85 \times 10^9)^{\frac{1}{4}}}{\left[1 + \left(\frac{0.492}{0.720538}\right)^{\frac{9}{16}}\right]^{\frac{4}{9}}} = 88.56$$

vii) <u>Coefficient of convection heat transfer</u>

$$Nu_L = \frac{hL}{k}$$

$$h = \frac{88.56 \times 0.027985}{0.588} = 4.215 W/(m^2.K)$$

viii) <u>Convection heat transfer at the Outer surface</u>

$$\dot{Q}_{Conv} = 4.215 \times 0.588^2 \times (93.4 - 24) = 101.13W$$

ix) <u>Total Convection heat transfer</u>

$$\dot{Q}_{Conv-Total} = \dot{Q}_{Conv} + \dot{Q}_{Cal} = 101.13 + 33.82 = 134.95W$$

x) <u>Heater's efficiency when mounted on the wall</u>

$$\eta = \frac{134.95}{391} \times 100 = 34.51\%$$

6) <u>Net radiation loss through the channel</u>

$$Q_{12} = \frac{\sigma(T_1^4 - T_2^4)}{\frac{1-\varepsilon_1}{A_1\varepsilon_1} + \frac{1}{A_1F_{12}} + \frac{1-\varepsilon_2}{A_2\varepsilon_2}}$$

60

$$\dot{Q}_{Rad-Chan} = \frac{5.67 \times 10^{-8} \times \left[(96.5 + 273.15)^4 - (47.4 + 273.15)^4\right] \times 0.588^2}{\left[\dfrac{1-0.76}{0.76} + 1 + \dfrac{1-0.76}{0.76}\left(\dfrac{0.588^2}{95}\right)\right]} = 97.48W$$

7) <u>Radiation loss at the outer surface</u>

The enclosure of the laboratory measured 5m x 3m x 5m (high)

The total surface area of the walls and ceiling (with the same emissivity) was:

$$A_{Enclosure} = 2 \times 3 \times 5 + 2 \times 5 \times 5 + 3 \times 5 = 95m^2$$

The form factor between the heater surface and the rest of the enclosure's wall is 1

$$\dot{Q}_{Rad-Outer} = \frac{5.67 \times 10^{-8} \times \left[(93.45 + 273.15)^4 - (24 + 273.15)^4\right] \times 0.588^2}{\left[\dfrac{1-0.76}{0.76} + 1 + \left(\dfrac{0.588^2}{95}\right)\dfrac{1-0.76}{0.76}\right]} = 152.95W$$

8) <u>Total radiation loss</u>

$$\dot{Q}_{Rad-Total} = 97.48 + 152.95 = 250.43W$$

9) <u>Total heat loss from the heater's surfaces:</u>

$$\dot{Q}_{Total} = \dot{Q}_{Conv-Total} + \dot{Q}_{Rad-Total} = 134.95 + 250.43 = 385.4W$$